UCLouvain

AGRO LOUVAIN BIOINGÉNIEURS

Faculté des bioingénieurs

Hydrogeophysical characterization of the soil along a floodplain-hillslope system in the High Fens

Author :	HENROTTE Sébastien
Supervisors :	Prof. LAMBOT Sébastien (UCLouvain/AGRO/ELI/ELIE)
	Prof. JONARD François (UCLouvain/AGRO/ELI/ELIE)
Readers :	Prof. VANACKER Veerle (UCLouvain/SC/ELI/ELIC)
	Prof. VANCLOOSTER Marnik (UCLouvain/AGRO/ELI/ELIE)
Academic year :	2021 - 2022
Bioingénieur :	sciences et technologies de l'environnement

Acknowledgements

Before starting this document, I would like to thank the people who made this work possible.

I would first like to thank my supervisors: professor Sébastien LAMBOT and professor François JONARD for giving me the opportunity to work on this fascinating project, for helping me on site and during the writing. I also thank postgraduate Maud HENRION for helping me throughout the project, on the field, for the processing of the data and for the writing. Thanks to postgraduate Yanfei LI for the drone-data acquisition on the site.

I would also like to thank the "Département dela Nature et des Forêts - Direction de Malmédy-Büllingen & Cantonnement de Malmédy" for giving us the authorization to work on the site. Also, thanks to ranger M. Manuel LEMAIRE for making sure that the field was accessible to us and that we had everything we needed on site.

I would like to thank my parents as well as my sister Sophie and my brother Tom for supporting me and helping me with the proofreading.

And finally, thanks to my friends Laura DECONINCK, Julien LEHMANN and Thomas FERDINAND, for supporting each other during the finalization of our master theses.

Contents

List of figures

1 Introduction

The term ”critical zone” was first used by the US National Research Council in 2001. It extends from the top of the vegetation canopy to the bottom of the fresh groundwater [13]. This zone provides a variety of services, such as food production, water cycling and climate regulation. The latter ecosystem service is especially significant for soils with high carbon content, such as peatlands, which act as important carbon stocks.

Despite the importance of the critical zone, the horizontal and vertical integration of its processes on the landscape level are not yet well understood because of the inaccessibility of the subsurface. Furthermore, the subsurface is rarely studied at a large enough spatial and temporal scale to identify the heterogeneities and occurring changes. This master thesis aims at studying and better understanding the subsurface of the critical zone with the use of hydrogeophysical methods. This project will focus on the integrated study of a natural peatland area in the Belgian High Fens. This master thesis is part of the LandSense project, whose objective is to clarify the critical zone in a multidisciplinary manner.

This document will start with giving a brief overview of the critical zone and of the ecosystem services it provides to human societies. It will then focus on the present situation of ecosystems as well as their management at the political level. This will be followed by a description of the general objectives of this master thesis and of the LandSense project. The study site will then be described. The methodology will then be described before presenting the results of the EMI, GPR and direct measurements. Finally, all these results will be discussed in an integrated manner.

2 General context

2.1 Soil and critical zone

2.1.1 Critical zone

The critical zone (CZ) is defined as "the Earth's permeable near-surface layer from the top of the trees to the bottom of the groundwater" [1]. It includes "land surface and its canopy of vegetation, rivers, lakes, shallow seas, and it extends through the pedosphere, unsaturated vadose zone, and saturated groundwater zone. Interactions at this interface between the solid Earth and its fluid envelopes determine the availability of nearly every life-sustaining resource"[14].

As represented in Figure 1, the CZ is composed of multiple envelopes such as the atmosphere, the biosphere, the hydrosphere and the lithosphere. These all play, in combination with the soil, a key role in maintaining the many ecosystem services within the CZ. [14]
The CZ is controlled by chemical, physical and biological processes that influence different cycles such as water, solutes, gases and sediments [15]. It also plays a critical role in the flux of nutrients that are essential for plants, such as N, P, K, Ca, Mg and S. Its many different functions make soils the basis of the food chains of the above ground biodiversity. [16, 1, 5].

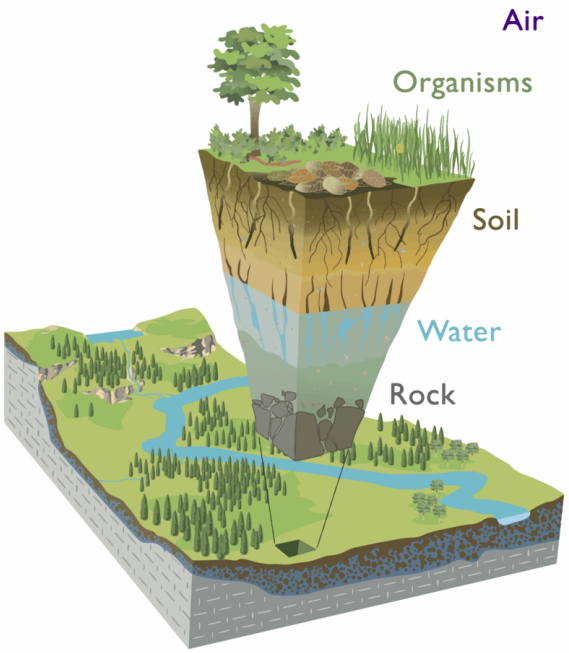

Figure 1: Critical zone extent [2]

The critical zone observatory program was created in 2005 and aims for multidisciplinary research of the CZ [17]. These observatories are located all over the world, in countries such as France, south-west China, Puerto Rico, Switzerland, USA, India, ... Each of these observatories may focus on location-dependent conditions such as karst environment, hillslope processes, glacial and periglacial environments, coastal environments, fluvial processes, ... [17, 18].

These initiatives increasingly recognize the importance of the integration of the above ground processes with the subsurface of the CZ. However, the subsurface is much more difficult to access and remains a key gap in the CZ knowledge. [1]

2.1.2 The soil

Soils are complex and dynamic ecosystems. It is in this complexity that resides the key to their role in supporting biodiversity [14, 19]. They serve as the main base for biodiversity on Earth

and are especially rich in terms of species: it is estimated that soils host more than 25% of the 1,5 million described living species worldwide [5, 19]. However, the vast majority of soil organisms remain unknown, as less than 10% of soil biota has been described. Furthermore, a soil characteristics and fertility are a combination of its mineral composition and the organisms it contains. A key functional role of soil biodiversity is its direct contribution to creating soil spatial structure. Indeed, soil organisms differing in size and function create soil structure and aggregates, which are hot-spots of microbiological biodiversity and activity. Soil structure is thus both a product and a cause of soil biodiversity. [19]

Soils play an important role in the water cycle, acting like a sink by filtering, absorbing and retaining water. They also play an important role directly in human food production systems, as 99% of all calories consumed by humans come from land-based ecosystems [14, 5]. They also heavily influence climate regulation, especially through their capacity to act like a carbon sink. The pedosphere contains about 1,500 Gt of organic carbon, it is twice the amount of CO_2 contained in the atmosphere (720 Gt) and up to three times the amount immobilized by vegetation (600 Gt) [14, 20]. Unsustainable use of soils can be a major source of greenhouse gas emissions [14, 20, 21].

The soil has the particularity of recording information about past processes and perturbations of the CZ. Indeed, perturbations can be from natural or human origin, understanding the geochemical and texture record (depth of profiles, concentrations, isotopic signatures, porosity as well as particle size and morphology) could help to predict responses of the CZ to human perturbations. [15]

2.2 Ecosystem services

Ecosystem services (ES) are described as being "the benefits that human beings derive from the ecosystem and are the medium by which the ecosystem functions are transformed for human well-being" [22].

The concept of ES has considerably gained in visibility and interest after the inception of the Millennium Ecosystem Assessment (MEA) in 2005 (see Section 2.3). This growing interest in the matter is shown in Figure 2, which shows the number of articles focused on ES published during the years following the MEA. There was a slight increase in articles relative to ES during the years following 2005. However, it is in 2012 that we observed the most important increase in publications, the following years continued the trend as the number of publications kept increasing year after year. [3]

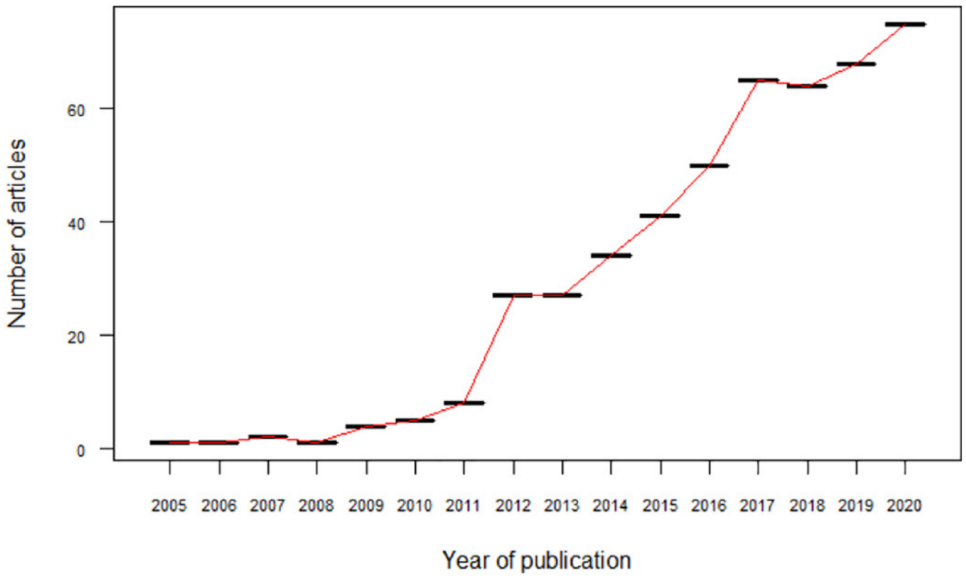

Figure 2: Evolution of the number of publications regarding ecosystem services since the release of the millenium ecosystem assessment in 2005 [3]

This graph shows the evolution of the interest of researchers in the concept of ES. This implies an increase in the attention given to the role of ecosystems and the understanding of their management. The maximization of human well-being ensues a better management of these ecosystems.

There are multiple classification schemes to classify ES. In most cases, four main ES categories are identified, which are: production/provisioning services, regulating services, habitat/supporting services and information/cultural services [14, 3, 23]. When it comes to soils, their health can provide as many of the following ES as possible [14, 5, 23, 16, 24, 4] if they are in good chemical, biological and physical conditions [5].

1. Support functions: These functions are essential and act as the basis of other soil ES such as the following.
    - *Biodiversity pool*: Provision of biodiversity, including habitats, species and genes.
    - *Nutrient cycling*: Moving of chemical elements through biotic and abiotic parts of the soil allows to maintain soil fertility.
    - *Soil formation*: Rocks and minerals are weathered by chemical, physical and biological processes.
    - *Water cycling*: Movement of water through the soil that affects the development of its biodiversity and functions.
2. Regulating services: These include regulation of ecosystem processes such as the following.
    - *Biological control of pests and diseases.*
    - *Climate and gas regulation*: Soils play a critical role in climate change. Soils capture and contain about 80% of all the carbon of terrestrial ecosystems.
    - *Hydrological control*: Regulation of water balance and protection against floods.

- *Filtering of nutrients and contaminants*: Protection of groundwater bodies.
- *Recycling of waste and detoxification.*

3. Provisioning services: Products obtained from ecosystems such as the following.
    - *Food and biomass production, including in agriculture and forestry.*
    - *Clean water provision.*
    - *Raw materials.*
    - *Physical environment.*
4. Cultural services: Non-material benefits people obtain from ecosystems through spiritual enrichment, cognitive development, reflection, recreation and aesthetic experiences such as the following.
    - *Heritage services.*
    - *Cognitive services.*
    - *Recreation services.*

Figure 3 shows the different links between ES and the most common constituents of well-being, according to the Millennium Ecosystem Assessment from 2005 [4].

It is important to keep in mind that the potential for mediation and the intensity of the linkage can differ depending on the region and the ecosystem. According to Aryal et al. [3], the most common ES treated in the literature is regulating services (37%). It is followed by provisioning services with 34%, supporting services with 19% and finally cultural services with 10%. More specifically, 53% of the literature selected in the review of Aryal et al. [3] was about carbon and climate services. It was followed by crops and grains (50%), biodiversity (34%) and water conservation and regulation (32%). These statistics show the importance of research on the topic of climate change, food security and the role ecosystems play in the balance of the benefits humans can take advantage of. This same review study also gives insight about the state and the focus of the research on ES by analyzing over 400 articles on the subject between 2005 and 2020. It shows the general lack of engagement of government institutions. Indeed, about 90% of these articles were based on funded research but less than 10% of these funding came from government institutions, weakening the policy linkage of the research findings [3]. This lack of involvement in research does, however, not mean that the governments are inactive. There seems to be a shift in governments where they now realize the importance of soils as well as the risks of their unsustainable management. A communication published by the European commission in 2021 states that grassland and cropland in the EU provide 76 billion euros per year, and less than one third of this amount comes from crop production, it mostly comes from other ES [5]. This shows how much soil quality is beneficial to society, even outside of food production. This indicates that the EU is becoming more aware of the risks and impacts of soil degradation on the economy and people's well-being. It is now trying to bring more attention from governments, parliaments, public authorities at all levels as well as economic operators,

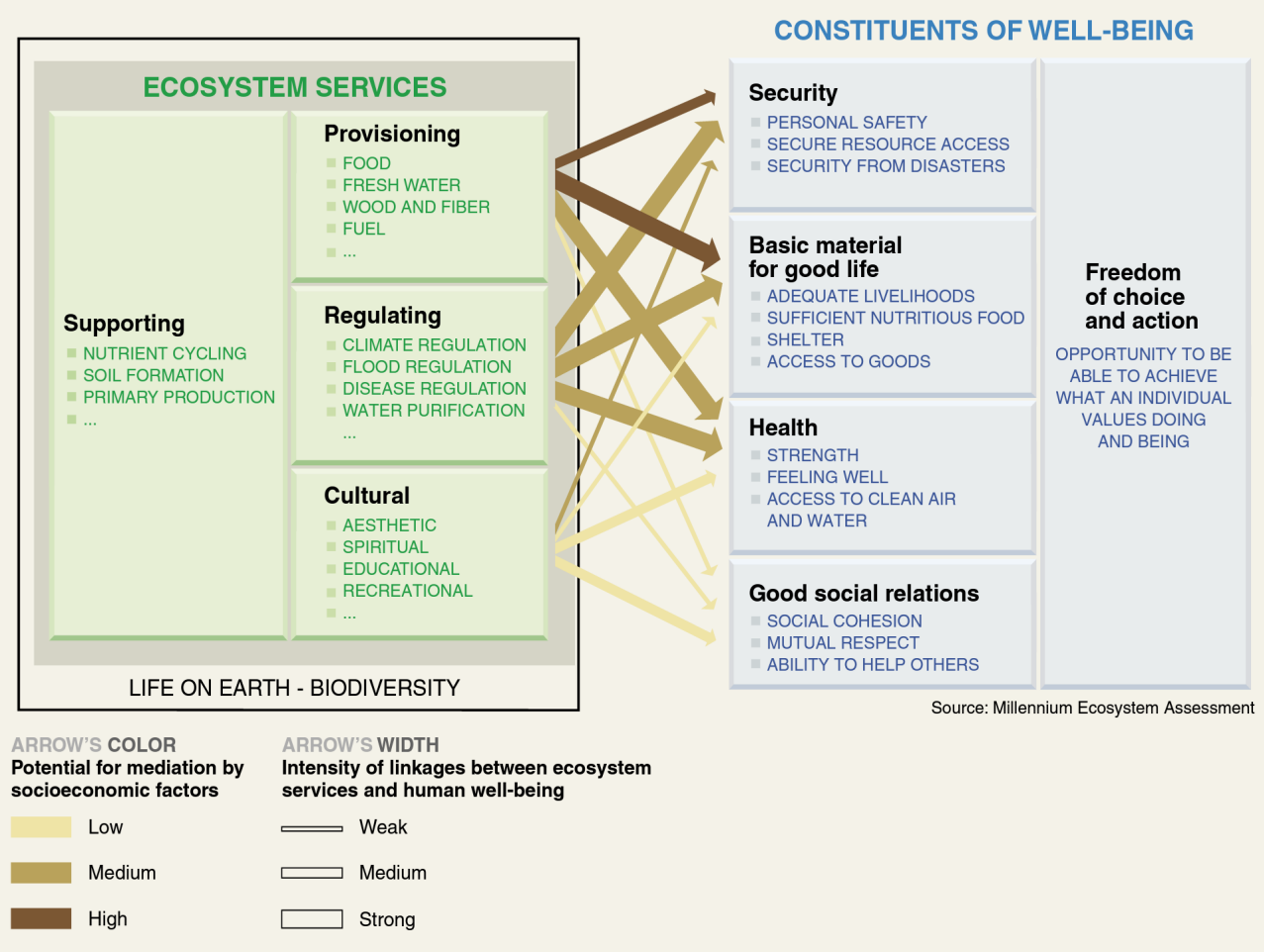

Figure 3: Link between ecosystem services categories and common constituents of human well-being [4]

soil users, local communities and citizens on the subject [5]. On 17 November 2021, the EU adopted the "soil strategy for 2030", this program aims to "set out a framework and concrete measures to protect and restore soils, and ensure that they are used sustainably. It sets a vision and objectives to achieve healthy soils by 2050, with concrete actions by 2030 [25]" as a part of the EU biodiversity strategy plan for 2030. This will be discussed in more details in Section 2.4.2.

The way and the frequency at which the land is used determines what ES a soil can provide. There may be a situation where the increase of an ES is only possible at the expense of another, this is called a trade-off situation [3]. This can happen according to two different perspectives. The first one is by *biophysical constraints*. It defines the production possibility frontiers (PPF) of the ecosystem assets to provide goods and services now and in the future. The PPF define the maximum rendering of one ES at each level of the other ES simultaneously, indicating optimal balance between two conflicting ES. The second trade-off perspective is *utility functions*: various stakeholders might have divergent values for the same ES which imply the trade-off in consumption and/or valuation of the ES. The most common trade-off relationship identified by the review of Aryal et al. [3] is between crops and grains in opposition to carbon and climate services. The second most frequent trade-off is opposing crops and grains production

with water conservation and regulations. It appears that the land use change and change in management objectives are the main driver of trade-off relationship, highlighting the critical role played by land users and management agencies. Expertise is thus of paramount importance for the sustainable management of ecosystems so that societies can benefit from them in the best possible way.

2.3 Present situation of ecosystems

The Millennium Ecosystem Assessment was released in 2005. it involved the work of over 1360 experts worldwide and had the ambition to assess the consequences of ecosystem change for human well-being. [26]

This assessment made four main findings [4, 26].

1. There has been a substantial and mostly irreversible loss of biodiversity on Earth over the past 50 years. This was caused by human activity to meet ever-increasing demand for raw materials such as food, water, fiber, fuel, etc. Increasing anthropogenic pressures lead to ecosystem losses, almost one quarter of Earth's terrestrial surface (24%) has been transformed.

2. These changes in ecosystems may have contributed to increasing human well-being, but they also have degraded many ES, increased risks of nonlinear changes and exacerbation of poverty for some groups of people.

3. The degradation of ecosystem services may worsen during the first half of the current century, thus being an obstacle to achieving the Millennium Development Goals.

4. Some scenarios provided by the MEA may allow for a reversing of the degradation of ecosystems, but would require serious changes in policies, institutions and practices.

2.3.1 Present situation of soil ecosystems

Poor management of soil health leads to the loss of some ES such as food security, flood mitigation, carbon sink as well as being a major risk for public health, etc. (see Section 2.2).

Multiple evidence point to the fact that soil resources are reaching critical limits and that the situation continued to deteriorate since the MEA in 2005. It is estimated that about 33% of soils are degraded [27, 16] and 24 billion tons of fertile soils are lost every year because of agricultural practices [28].

The situation is dire in Europe as well. EU soil patrimony is extremely rich, out of the 32 world main soil groups, we count 24 on the European territory [29]. This richness is however threatened as it has been estimated that between 60% to 70% of the soils of the EU are unhealthy. Furthermore, 1 billion tons of European soils are lost every year because of erosion [5]. There have been directives concerning air [30], water [31], biodiversity [32] but the EU has

been unable to equip itself with an adequate legal framework granting soils the same level of protection as water, marine environment and air for a long time, this will be further discussed in Section 2.4.2 [5].

In the Intergovernmental Science-Policy Platform on Biodiversity and Ecosystem Services (IPBES) "Global Assessment on Biodiversity and Ecosystem Services", it is estimated that around 12 million hectares of land are lost each year to degradation, which is harming the well-being of 3.2 billion people. Land degradation costs more than 10% of annual GDP because of loss of ES [6].

2.3.2 Soil degradation processes

There are different types of soil degradation that have been identified by the Food and Agriculture Organization (FAO) [33]. These are loss of organic carbon, water and wind erosion, acidification, pollution, waterproofing, compaction, nutrient imbalance, salinization and biodiversity loss.

However, soil threats can be better classified in one of three categories

- *Physical degradation*: compaction, waterproofing, water availability, erosion and desertification.
- *Chemical degradation*: salinization, contamination, acidification, fertility loss, alkalinization.
- *Biological degradation*: loss of biomass, loss of biodiversity, biological invasion, loss of organic matter stock.

These kinds of degradation can harm the richness of some soils, including natural resources, as well as soil ES and functions. This, in turn, hurts biodiversity, environmental health and ultimately human well-being. [27]

2.3.3 Soil degradation drivers

These different kinds of degradation are exacerbated by some drivers. They operate at various spatial and temporal levels in society and comprise factors that bring socio-economic and environmental changes. These differ from one region to another, within and between nations. Drivers are diverse in nature and include: demographics, economic factors, scientific and technological innovation, markets and trade, wealth distribution, institutional and sociopolitical frameworks, value systems and climate change. [34, 35].

In their book "Drafting legislation for sustainable soils: a guide", Hannam et al. [36] have identified 3 main drivers that determine the rate of degradation. These 3 main categories of drivers are

- *Biophysical*: land use and land management, including deforestation and tillage methods. This is influenced by education and cultural values [27, 36].

- *Socio-economic*: human population is expected to increase by 33% between 2015 and 2050 [27], thus increasing pressure. The urbanization trend is expected to increase. In 2014, 54% of the world population was living in cities, whereas it is estimated to increase to 66% by 2050.
  Marketing and the rising demand for some products influence land use. The most notable of these drivers is the reduction of forest cover in favor of crop production and livestock [34].

- *Political forces*: Political ideology, such as policy responses to climate change. One notable example of this is the offsetting of emissions in the industrialized north by protecting forests in the south [27]. Another example is the relocation of some large stationary greenhouse gases sources from developed countries to other parts of the world [34].

2.3.4 Soil degradation causes

There can be one or multiple causes for each type of soil degradation process. These causes are a menace for soil to achieve its role for life on Earth [16]. Some of the most important ones are:

- *Mismanagement of cultivated arable soils* by the improper use of fertilizers, poor quality of irrigation water, inadequate maintenance of the soil, use of heavy machinery etc. This can lead to accelerated erosion, compaction, loss of nutrients, salinization and soil pollution.

- *Removal of natural vegetation* is one of the most important environmental concerns. The clearing of forests and other natural ecosystems in favor of agricultural parcels destroys biodiversity and make soils more vulnerable to water and wind erosion [36, 37, 22].

- *Over-exploitation of vegetation for domestic use*, this includes activities such as excessive gathering of fuel-wood, fodder and unsustainable timber extraction.

- *Overgrazing* results in loss of vegetation cover and soil compaction, it predisposes soil to water and wind erosion. [36, 22, 4].

- *Industrial activities* are often linked to soil pollution, soil waterproofing and loss of soil productivity.

The largest greenhouse gases emissions from soils are resulting from degraded land as well as land use change. One of the most notable and important land use changes regards the drainage of organic soils, which amounts to a yearly release of 20-40 tonnes of CO_2 per hectare. The most effective option to manage soil carbon in order to mitigate climate change is to preserve the existing stocks of soils [21, 16].

As a result of these findings, the MEA has considered several scenarios, some of which would allow for the reversing of the degradation of ecosystems. These would however require important changes in policies, institutions and practices [4].

Hannam et al. [36] suggest different legal and institutional elements as basic and essential components of a way to promote actions for the achievement of the sustainable use of soil. These can be used as a way to assist in assessing the capacity of an existing instrument to meet prescribed standards of performance for the sustainable use of soil. It may also be used to guide the reform of an existing soil law, or to develop new legislation for the sustainable use of soil.

2.4 Political measures

2.4.1 Measures taken in Wallonia

In 2008, the first decree regarding soil management in Wallonia, the "décret relatif à la gestion des sols" was published. Its objectives were to prevent the depletion of soil, as well as soil pollution remediation [38].

A new version of this decree was voted by the Walloon Parliament in 2018. It still follows the ideas of the decree from 2008 through preserving and improving soil quality, prevention of soil depletion and identifying soil pollution sources. Its first callings are environmental and sanitary through depollution of polluted soils, but it also aims at putting brownfields and contaminated soil back in the economic circuit [39, 40].

2.4.2 Decisions of the Commission of the European communities

Land is a finite resource, and the way it is used is one of the most important drivers of environmental change (see Section 2.3.3). The main factors influencing land use identified by the European Environment Agency (EEA) [24] are the increasing demand for living space per person as well as the link between economic activity, increased mobility and the growth of transport infrastructure, which usually result in urban expansion. The EU has recognized the fact that the degradation processes of the soil are significantly increasing due to rising anthropogenic pressures and may worsen in the future if no action is taken. Every year, about 1 billion tons of soil are washed away by erosion on EU territory [41]. On a net basis, over 400 km^2 of land were taken each year in the EU between 2012 and 2018. Land loss by urban areas and infrastructure is generally irreversible. It results in soil sealing, areas covered by artificial surfaces lose all their resources and are only able to support few socio-economic and housing functions. The main drivers of land take during 2000-2018 were industrial, commercial, extension of residential areas and construction sites [24].

Soil degradation will have an impact on sustainability and long term competitiveness in Europe. The eight main threats to soil identified by the EU are erosion, organic matter decline, contamination, salinization, compaction, soil biodiversity loss, sealing, landslides and flooding. This impacts water quality, human health, climate change, nature and biodiversity protection

as well as food safety [42].
It is in the hope of mitigating those risks that in 2006, the European Parliament and the council proposed the establishment of a **framework for the protection of soil** [43] since there was no specific Community legislation on soil protection at the time. The goal of this directive is to ensure the fact that the soil will be able to be protected and keep its environmental, economic, social and cultural functions [42] or in other words, its ES 2.2.

The European directives for the protection of soil will be updated as a part of the **EU Biodiversity Strategy for 2030** [23, 5, 32]. The objective is to establish a larger EU-wide network of protected areas on land and seas, by enlarging Natura 2000 areas as well as launching a EU nature restoration plan [32]. The main actions it aims to take are the following:

- Establishing a larger EU-wide network of protected areas on land and sea.
- Launching a EU nature restoration plan.
- Introducing measures to enable the necessary transformative change.
- Introducing measures to tackle the global biodiversity challenge.

The EU Biodiversity Strategy for 2030 [32] is focused on more than 100 actions that EU Member States are committed to implement by 2030. Out of all these action, 23 have been completed, 73 are in progress and 8 are delayed.

Figure 4 represents the 5 actions of the EU Biodiversity Strategy for 2030 that are specifically focused on soil, we can see that one of them is already completed. It is the EU Soil Strategy, which was adopted in November 2021. The EU Soil Strategy aims to ”tackle in a comprehensive way soil and land degradation, as well as to fulfill EU and international commitments on land degradation neutrality”.

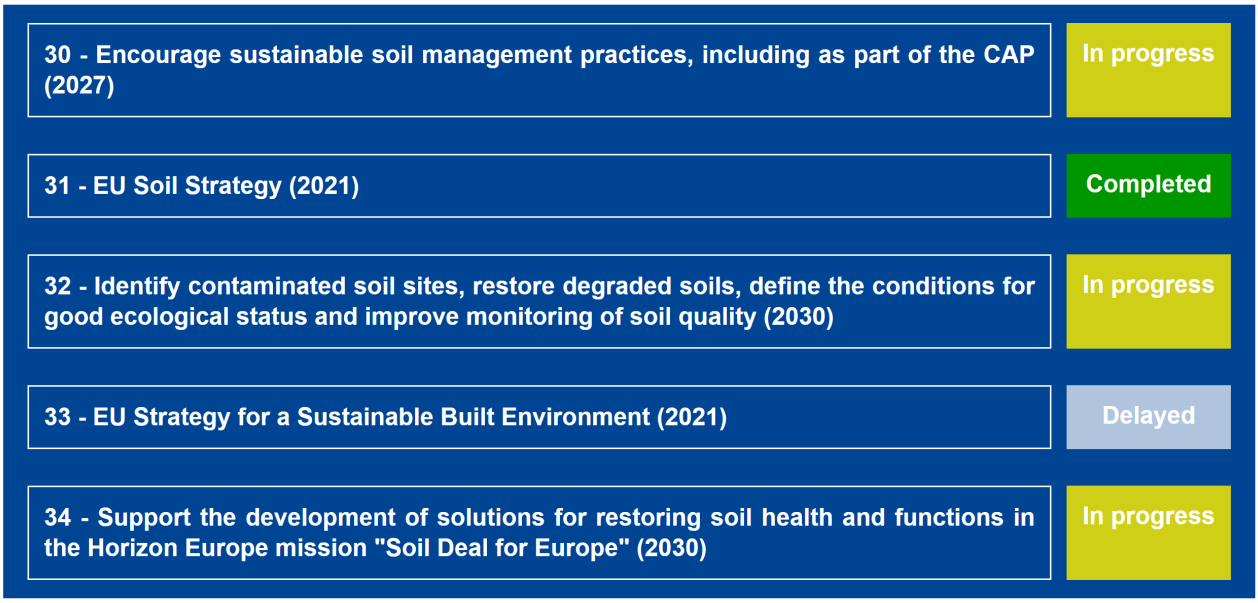

Figure 4: Progress of the actions from the EU Biodiversity Strategy for 2030 specifically focused on soils

The **EU soil strategy for 2030** [5] aims to protect and restore ecosystems so that by 2050, all EU ecosystems are in healthy condition [25] with concrete actions by 2030. The objective of this strategy is to set out a framework and concrete measures to protect and restore soils, and ensure that they are used sustainably [25]. It is a key deliverable of the EU biodiversity strategy for 2030 and will play a role in the achievement of the objectives of the European Green Deal, which has the ambition of transforming the EU into the first carbon-neutral continent by 2050 [44].

Figure 5 illustrates the direct links and synergy between the EU Soil Strategy [5] with multiple other EU policies emerging from the European Green Deal such as the Biodiversity Strategy for 2030 as well as the Rio conventions and SDGs (see 2.4.3). Figure 5 suggests the emergence of a new trend where soils are getting more attention and are explicitly linked with other initiatives by the EU.

The medium-term objectives for 2030 of the EU Soil Strategy [5] that are directly focused on soils include combat desertification, restoration of carbon-rich ecosystems as well as removing of 310 million tonnes CO_2eq per year for land use, land use change and forestry. It also includes reducing nutrient losses, making significant progress on remediation of contaminated sites, as well as reducing use and risk of chemical pesticides by at least 50%.

On the longer term, the objectives are to reach:

- No net land take.
- Reducing pollution to a point where it is no longer harmful for human health and ecosystems.

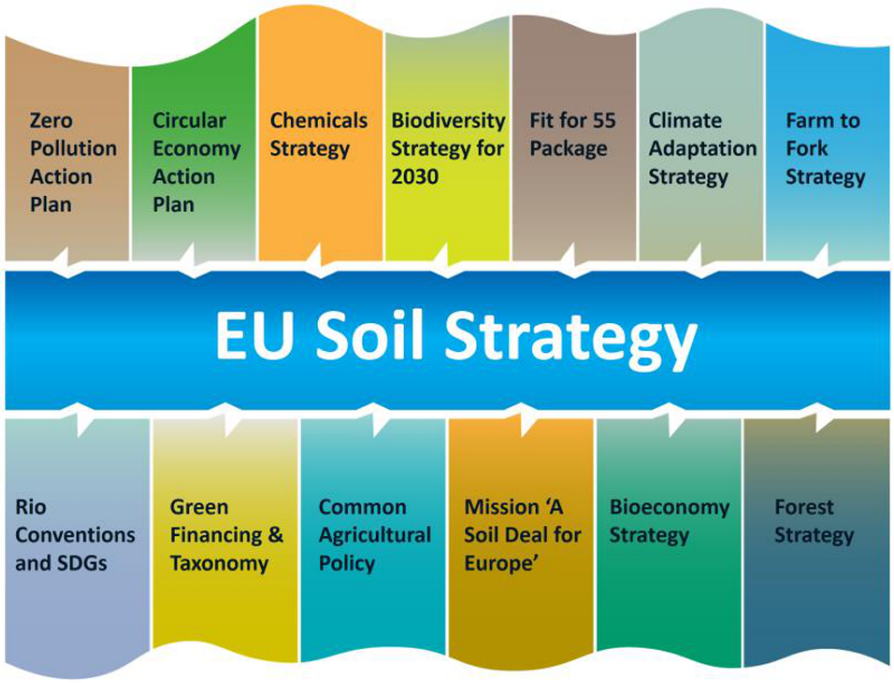

Figure 5: Link between the EU Soil Strategy and other EU initiatives [5]

- Achieving climate-neutral Europe by achieving land-based climate neutrality by 2035.
- Achieving for EU a climate-neutral society, adapted for the unavoidable impacts of climate change by 2050.

2.4.3 Sustainable development goals (SDGs)

The MEA allowed for the establishment of the Millennium Development Goals (MDGs) in 2008 [45]. The objective was to give some political input to catalyze the understanding of the importance of meeting the 8 MDGs. Unfortunately, most goals ended up forgotten or ignored [45]. It was then decided to implement new objectives in 2015, to replace the MDGs, in the hope of reaching more people. 2015 being the last target year of the MDGs was a perfect starting point for the SDGs, which apply to both developing and developed countries, following where de MDGs left off for the 2015-2030 period [45, 37].

These goals have been formulated and adopted by all 193 countries of the United Nations (UN) [46]. However, it is claimed that these SDGs have not paid enough attention to the importance of soils [37, 47, 48, 23]. Soil scientists were not represented on the committees charged with the formulation of the SDGs, nor on the committees setting targets and indicators [47, 48]. The presence of these experts is essential, knowing how much human society relies on soils. Indeed, even though some SDGs have targets which take soil resources into consideration, not a single SDG is directly focused on soils nor does any directly use the term "soil" [47, 48, 23]. SDGs regarding food security (2 and 6), food safety (3), land-based nutrient pollution of the sea (14), urban development (11) as well as mitigation and adaptation to climate change (13) do include soils in their directives as an indirect factor regulating these goals. There is an urgent need

to assess and monitor soil properties that impact soil productivity. Especially on the following properties: nutrient status, pollution, soil organic carbon (SOC) changes, hydraulic properties and soil biodiversity. Tóth et al. [47] conclude that the monitoring of progress in soil resources protection and sustainable soil-based development can not be done without a global indicator framework. They also conclude that policies have to consider the spatial extent of global and regional soil quality assets, ranging from sustainable urbanization to agricultural development.

Soils may however take a more important part in the SDGs in the future. While the SDGs and their targets have been finalized, the indicators of some goals are still being discussed. Indeed, each SDG has a number of targets, but the indicators are not always clearly defined. This is why each goal is classified into one of three tiers [47, 48].

- Tier I: The indicator is conceptually clear and has an internationally established methodology. Data is regularly collected for at least half of the countries where the indicator is relevant.
- Tier II: The indicator is conceptually clear and has internationally established methodology, but data is more scarce than in Tier I.
- Tier III: The methodology and/or standard of the indicator are being (or will be) developed or tested.

The objective is that tier II and III objectives eventually move to tier I. An opportunity for soil science to be acknowledged in the SDGs resides in Tier III indicators. Indicators that include soils are (or will be) discussed, and there are possibilities for new soil-oriented indicators to be explored. For that to happen, soil scientists will need to express the dynamic role of the soil by applying simulation models of the soil-human-climate-plant system. It will also be necessary to define spatial patterns of soil behavior, and finally it will be necessary to quantify the interrelationships in the integrated soil, water, atmosphere and plant systems for soil-based SDGs [47, 48].

The greatest strength of the SDGs is that they provide a widely known and supported policy roadmap to achieve sustainable development. Soils may be more represented in the future if the soil science community actively participates by showing the relevance of soil science in SDG research as well as indicators.

Figure 6 is the result of a study conducted by the IPBES. It presents the results of a survey of 13 coordinating lead authors of the ”assessment report on land degradation and restoration” [6]. These authors were asked to synthesize findings of the assessment to evaluate the relevance of land degradation in regard to targets of each SDG, as well as the extent to which addressing land degradation would have a positive or negative impact on progress towards each SDG.

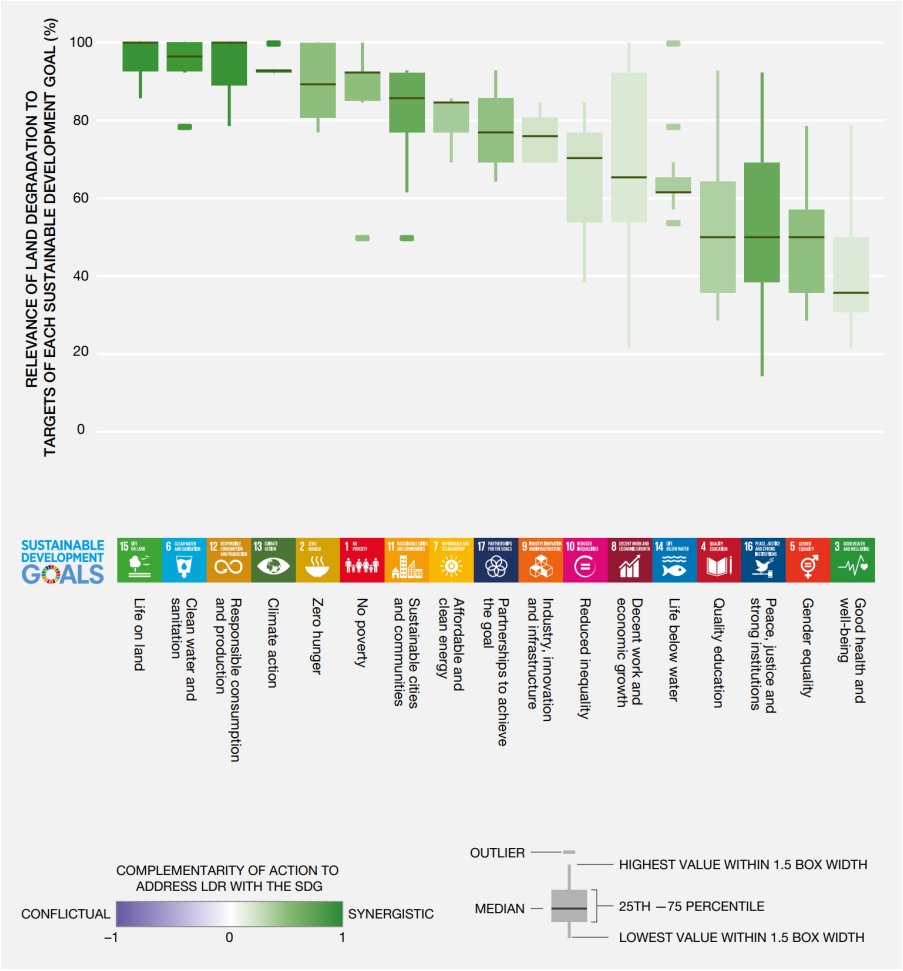

Figure 6: Relevance of land degradation to targets of each SDG [6]

The vertical axis indicates the percentage of experts who believe halting land degradation and restoring degraded land to be relevant to the achievement of each Goal. The green colors indicate the degree to which the targets are synergistic with progress to address land degradation. We can see that all the categories are shades of green, which means that the relationship between efforts to address land degradation and meeting the SDGs are never judged to be more conflictual than synergistic

Based on what is represented in Figure 6, we can conclude that assessing land degradation is never detrimental to the SDGs and is even essential for reaching the majority of them as well as delivering co-benefits to almost all of them.

2.5 Peat soils

Peat is a soil material consisting of at least 30% of dead organic material, in dry mass [49, 7, 5]. They form after the deposition and partial decay of vegetation in wetlands in anaerobic conditions due to chemical, biological and enzymatic processes. These processes are mostly due to the action of bacteria, fungi and chemical compounds of plant remains [49]. Peatlands are found around the world: in permafrost regions close to the poles and at high altitudes, in coastal areas, beneath tropical rainforest and in boreal forests [50], as shown in Figure 7.

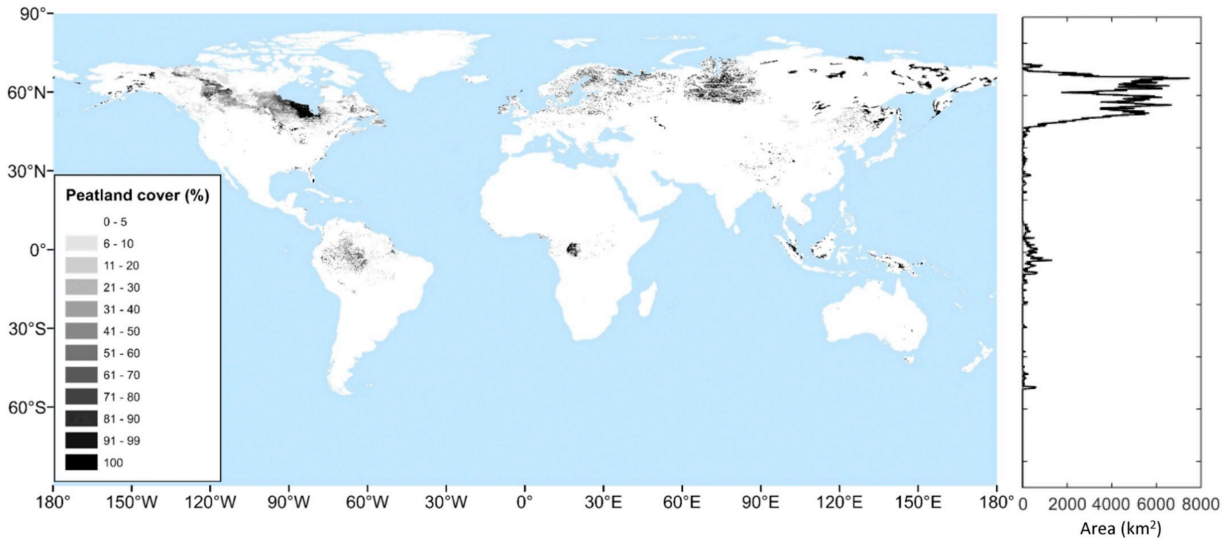

Figure 7: A global estimate of peatland distribution around the world [7]

These types of soils are characterized by low pH. This is due to the colloidal peat molecules, the surface of which is covered with functional groups carrying negative charges. These charges result in the binding of positive hydrogen ions. Unbound hydrogen ions account for the acidity of the peat, whereas the bound hydrogen is considered potential acidity [51]. These types of bound and unbound protons are in equilibrium, which means that when free hydrogen molecules are neutralized, hydrogen from the potential acidity will be released. When this happens, the newly unbound hydrogen ions will be replaced by other positively-charged ions such as Ca^{2+}, Mg^{2+} and Na^{+}, this is called ion exchange. The total amount of all positive charges or cations absorbed by the peat is called cation exchange capacity (CEC), which is a function of pH [51].

Peatlands provide many important ES such as water purification and flood prevention. They are also rich in terms of biodiversity and also provide recreational opportunities on a cultural ES level [52, 53, 54]. One of their most important ES is regulation. Peatlands have a globally important role in carbon storage [52, 53, 54]. They may cover less than 3% of the global land surface, but it has been estimated that they contain between 5% to 20% of the global soil carbon stock [7]. The most important threat that causes the release of greenhouse gases in peatlands is drainage [55, 50]. Peatland drainage across all land categories in Europe alone emits around 5% of total EU greenhouse gases emissions, even though they cover less than 8% of its surface [5]. The land use change and especially the drainage amount up to 20-40 tons of CO_{2eq} per hectare per year [21]. Peatlands are drained for agriculture, forestry, but peat can also be used for horticulture or energy production [50, 52]. This impact is visible in Belgium as the peatland covered surface has considerably decreased over the years. It has been estimated that originally, peatlands may have covered between 20 000 to 70 000 ha, which represents between 0,65% and 2,28% of the total surface of the country [8]. Today, 13 000 ha of peatland remain in Belgium, only 300 of which are still active [8]. Their locations are shown in Figure 8

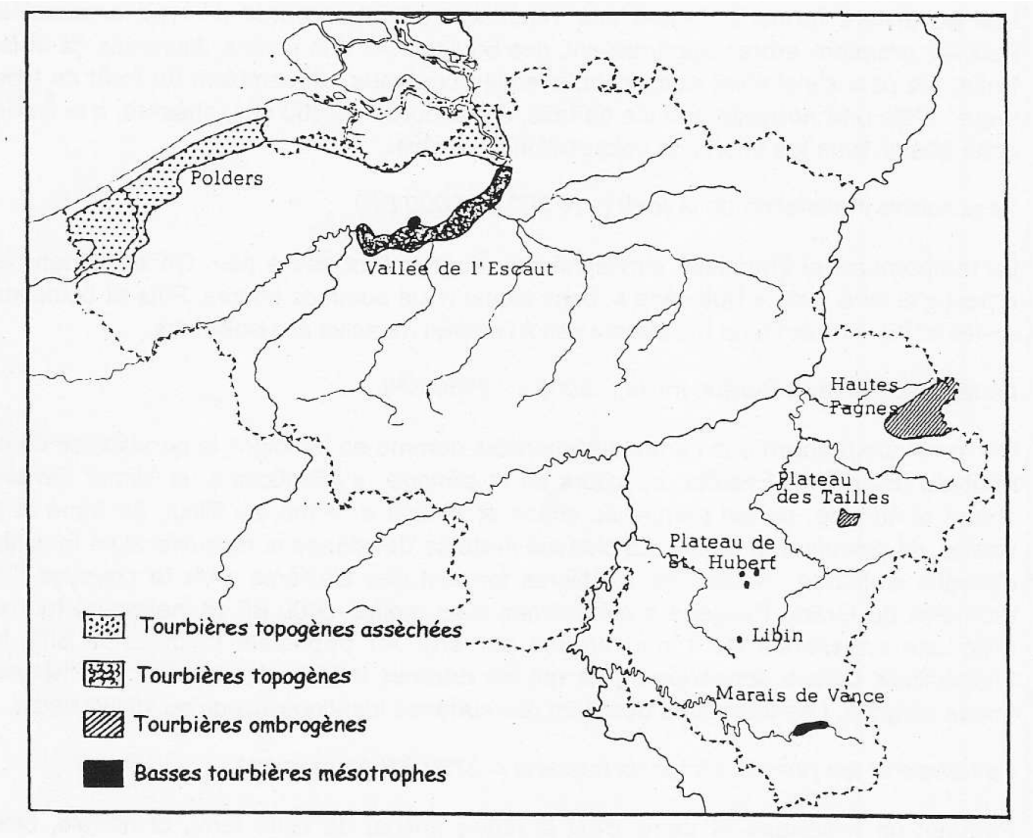

Figure 8: Peatland locations in Belgium [8]

Restoring drained organic soils alone could have a significant impact on the reduction of greenhouse gases emissions from terrestrial environments, this would be beneficial on multiple levels, such as nature, biodiversity and water protection [5, 21].

Peats have noticeable qualities when it comes to the utilization of geophysical techniques such as GPR and EMI because of their saturated mass, net negative surface charge, high cation exchange capacity and high specific surface area [49]. A geophysical study conducted in the High Fens by Schumacker et al. [56] in 2002 also praise the effectiveness of radar use in peatlands. Schumaker et al. [56] stated that the high water content and low electrical conductivity of peatlands make them especially favorable to the use of radar. This makes the chosen study methods appropriate for a peatland analysis.

3 General objective

As previously discussed, the critical zone (CZ) represents a fundamental part of the way the whole Earth system functions. The subsurface is difficult to access and remains a key gap in the CZ knowledge (see Section2.1.2). This is one issue the LandSense project (see Section 3.1) aims to address with the use of non-invasive sensing techniques.

The goal of this thesis will be achieved in the form of a case study in the High Fens, in eastern Belgium. This will be done through the integrated use of multiple geophysical techniques and sensing methods, such as electromagnetic induction (EMI), on-ground and drone-borne ground penetrating radar (GPR) as well as drone imagery. The data gathered by the use of geophysical techniques will be interpreted with the help of direct measurement and observations such as conductivity probes and soil profiling.

The objective of this study is to **characterize the subsurface of the CZ of a study site in the Belgian High Fens using geophysical techniques**.

3.1 The LandSense project [1]

LandSense is a research project led by Jonard François, Lambot Sébastien, Opfergelt Sophie, Vanacker Veerle and Van Oost Kristof. The project aims to ensure a better understanding of the CZ. The overarching research question of which is: **What are the hydrological controls on soil processes controlling carbon- and nutrient-efflux in the CZ at the landscape scale?**

Recent technological advances and technologies available to the LandSense research project provide a variety of tools to analyze the research field. Amongst those technologies are GPR, EMI as well as multi- and hyperspectral remote sensing. All these techniques allow for an integrated study of the field, as well as a much more complete picture of the CZ by vertically and horizontally integrating both surface and subsurface. LandSense aims to advance CZ research by combining these multi-sensor approaches with carefully designed field surveys and advanced modelling approaches.

The first phase of the project aims to develop the integration of spatially continuous sensing and point-based field approaches. This will be applied to carbon and nutrient fluxes study in Belgium, more specifically, on a hillslope-floodplain system. This master thesis falls within this first phase, whose ultimate goal is to "develop the integration of spatially continuous sensing and point-based field approaches". However, this thesis will focus on spatially continuous sensing as the installation of point-based sensors being intended later in 2022 or 2023.

4 Study site

4.1 Location

The site is located in a natural area of the High Fens, in the eastern part of Belgium and more specifically, in the northern part of the commune of Malmedy. It appeared that the west side of the road (beyond the western limit of the current study site represented in Figure 9), which had originally been planned for measures, was not really fitting for the kind of measurement we planned to do. Trees were planted and surrounded by iron fences to protect them from herbivores. This turned out to be problematic for two reasons. First, the trees and the fences were already 2 or 3 meters high, which could be dangerous for low altitude drone flights. Second was the fact that it is very likely that the metallic fences would interfere and distort the results obtained by EMI (see Section 5.2), as it is very sensitive to metal and other highly conductive materials. We then chose to map the east side of the road, delimiting a study site perimeter that is about 900 by 350 meters. On the southern part, there is a plateau and on the northern side of the road, there is a gentle hillslope going all the way down to the river as illustrated in Section 4.2. The topography, roads and vegetation led us to split our study site into 3 different parts, as illustrated by Figure 9.

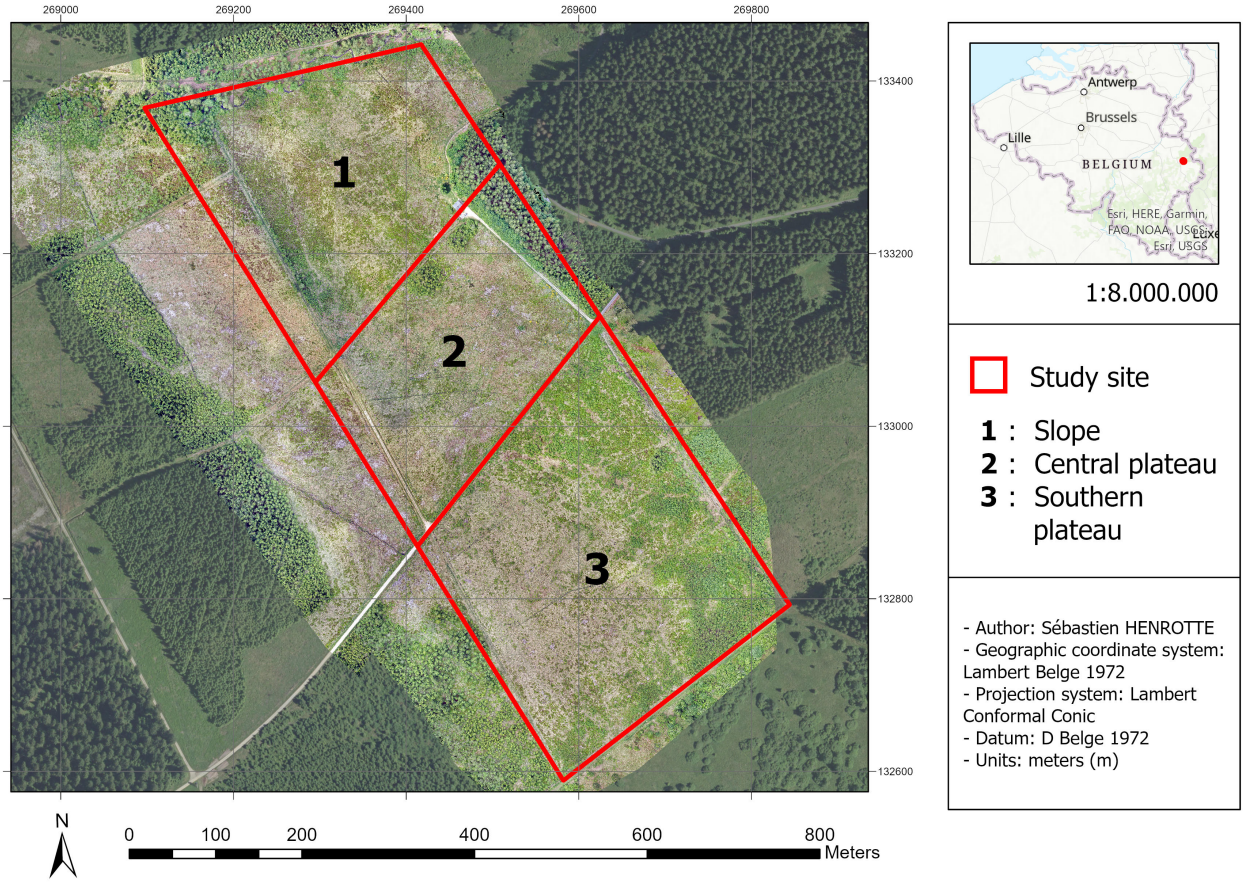

Figure 9: Orthophoto of the study site, separated in 3 distinct zones, realized by postgraduate Li Yanfei on June 6th 2022. The background is an orthophoto from 2017 and comes from the WalOnMap site [9]

From north to south, these three areas will, respectively, be called ”slope”, ”central plateau” and ”southern plateau”, in the remainder of this document. This decision was made because each area seemed fairly different on multiple levels. First is the topography that will be discussed in the following Section 4.2. Second is the presence of two roads and the deep drains that were dug on both sides of each of them. This heavily disrupts the surface and shallow hydrology, which is a key focus of this study.

4.2 Topography

The High Fens are a plateau that hosts the highest point of Belgium, the ”Signal de Botrange” (694 meters), which is only a couple kilometers away from this site. We can see on the map from Figure 10 that the altitude of our site is not very different from the ”Signal de Botrange”. The peak of our study site culminates at an altitude of 635 meters and is located is the south-east corner of our study perimeter. The lowest altitude point of the study site is located on the opposite corner, in the north-west, with an altitude of around 590 meters.

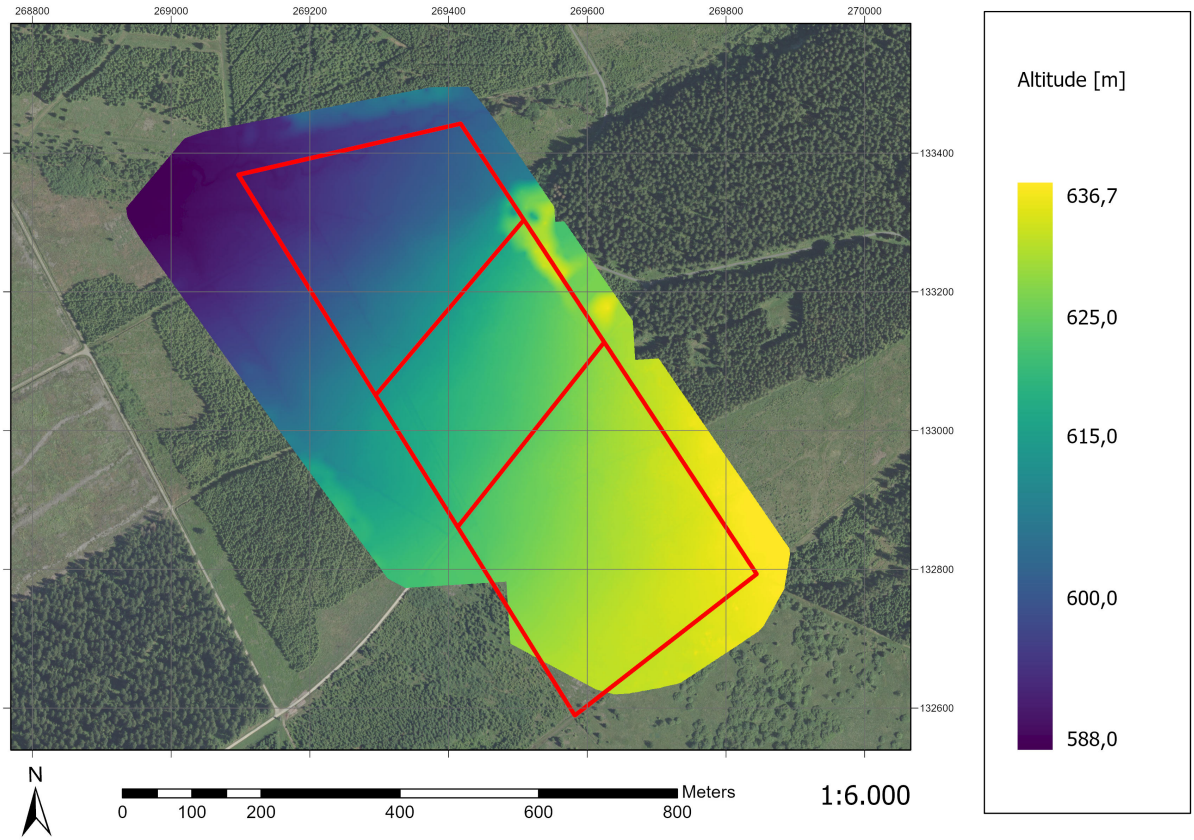

Figure 10: Study site topography

Starting from the river, going north to south, we first have the slope going up towards the south-east until it reaches a trail that marks the limit between the slope and the second area. The southern half of the central plateau is populated with young trees that are surrounded by metallic fences. This area extends to the main road, which marks the limit between the central plateau and the last area. South of this road, we have the fenced plateau with denser

vegetation, especially towards the eastern part. We can see in Figure 10 that the central and southern plateau area are relatively flat.

This kind of system is interesting because the topography plays an important role on surface as well as subsurface fluxes. We are thus expecting to observe different results between the different areas.

4.3 Pedology

As seen in the soil type map of "WalonMap" [9] illustrated in Figure 11, the soil of the study site is very rich in organic matter and is mostly classified as "peatlands".

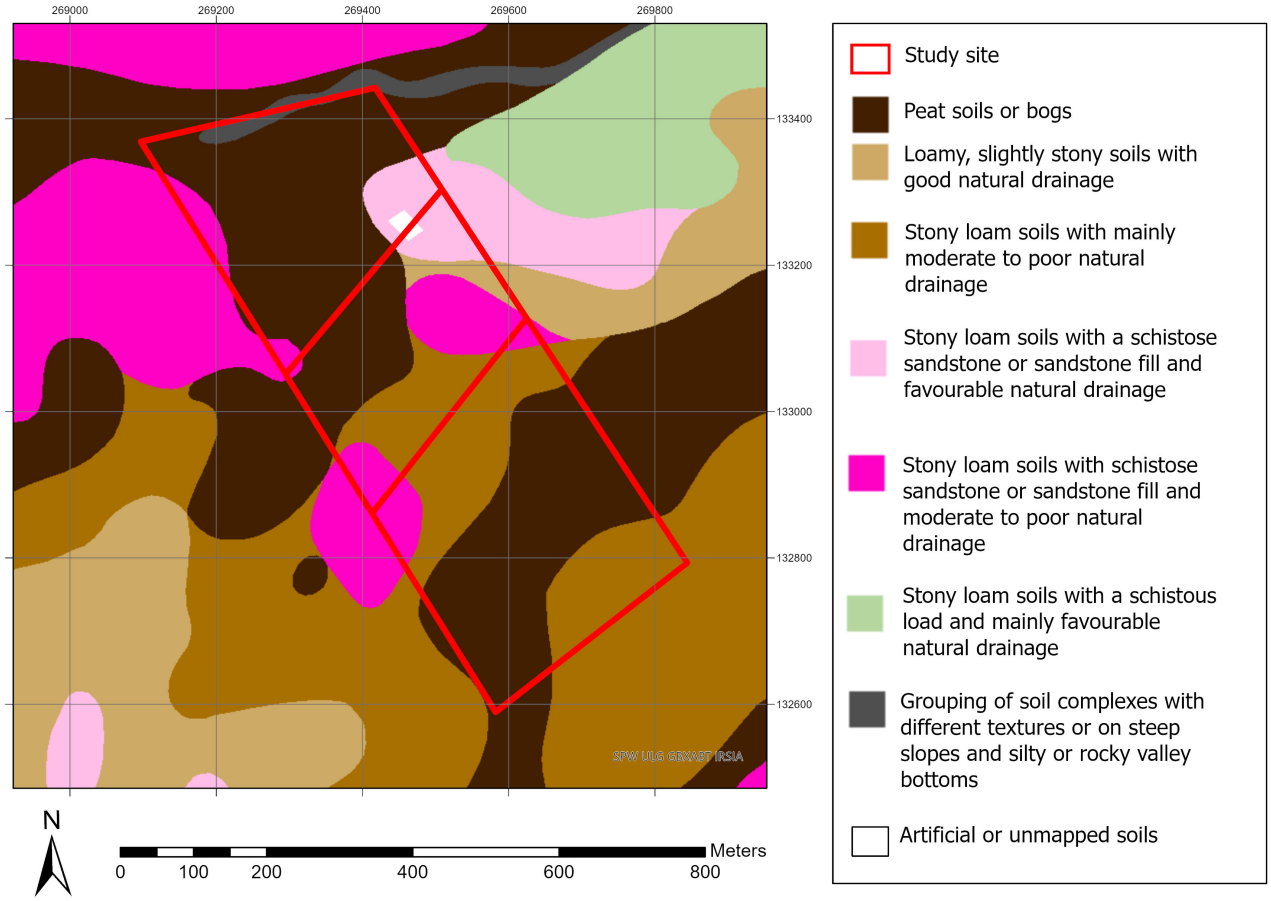

Figure 11: Main soil types covered within the study site [9]

Figure 11 shows that soils are mostly composed of loam and peat. However, after a few on-site studies, it appeared that the peat layer is present on all of the study site with varying depth. The three different parts of the study site presented in Figure 9 are shown in Figure 11 to emphasize the fact that, according to the pedology map from WalOnMap, one same area may be comprised of multiple soil types. The information displayed on this map will be further discussed later on in this document.

Some drains are still clearly visible in our study field, as it is not uncommon in the Belgian High Fens. It is thus likely that the organic matter is fairly humified as it was exposed to aerobic

conditions following the drainage. Our first observations on the field have shown that the peat of the study site is well humified, as it was very homogeneous with very few distinguishable and identifiable organic matter fragments. However, the soil profiling (see Section 6.3) revealed that the peat was not as homogeneous as we first thought, as some fragments of vegetation, mostly wood pieces, were still distinguishable in some profiles.

4.4 History

The study site is located in the High Fens, which is a region of Belgium located on the north-eastern part of the Cambro-Ordovician Stavelot-Venn massif [57, 56, 58]. This massif lies on quartzite and slate bedrock and has been revealed to be of important biological and geological interest, which has led to the creation of the largest nature reserve in Belgium: the High Fens Natural Park, which covers an area of 4500 ha [58]. The High-Fens plateau has a relatively flat topography and is the highest point of Belgium, with its peak reaching an altitude of 694 meters at Botrange [57, 56].

The High Fens are mostly composed of forests and bogs. Peat deposits started to develop during the beginning of the Holocene era, more specifically during the Preboreal period (9400 - 8100 BC.) and may even have started at the end of the Pleistocene period [56, 57].

The comparison of the map of Ferraris from the end of the XVIIIth century with more recent maps shows that the area covered by fens has considerably decreased, especially between 1875 and 1925, decreasing from 15 000 to 5 000 ha [59]. In the past, the High Fens were much more exploited by the people of neighboring regions, especially in the form of agriculture such as grazing, mowing, cutting of coppice and timber, charcoal burning, grubbing and clearing [56, 59]. These practices have led to deforestation and to the emergence of large moors areas. It was very common to practice reforestation by planting spruce, which are not adapted to humid soils such as the ones in the High Fens. They thus required a tight network of drains to be able to grow in the region. This has led to important disruption of equilibrium in the ecosystems of the region [59]. Today, the forest landscape is especially occupied by common spruce, whereas the moors and bogs are occupied by an invasive type of grass: *Molinia caerulea* [56]. One other activity caused massive drainage of the soil: the extraction of peat to be used as fuel also required the soil to be drained beforehand [59, 56]. These practices have heavily altered the High Fens landscape, as well as releasing considerable amounts of greenhouse gases in the atmosphere [16, 21].

The Natural Park of the High Fens is currently following the management plan "Hautes Fagnes-Eifel". In this plan are all the guidelines that will be followed for the 2016 to 2026 period to ensure the protection of the park's rich patrimony, while keeping it open to the public [60].

For management purposes, the general area of the location of the site is divided into multiple compartments. The study site covers a large area that expands on multiple compartments represented in Figure 12, each having their own history and management.

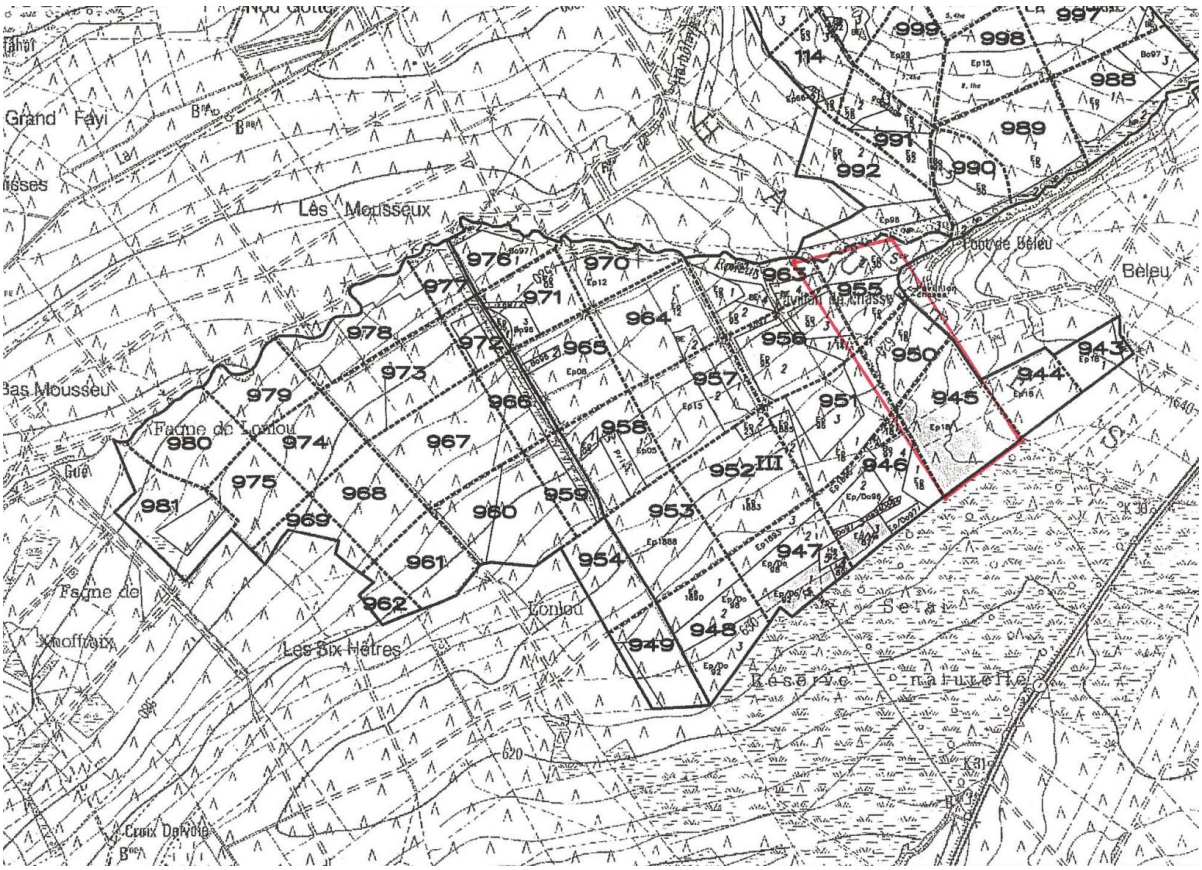

Figure 12: Distribution of the compartments of the High-Fens State Nature Reserve prior to 2017, 2018 [10]

The zone of interest for the LandSense project covers 3 major zones: *945*, *950*, *955* as well as small portions of zone *963*, *956* and *951*. We will however focus on the three main compartments, as these are the ones that have been selected for our final transects after a few tests.

- Compartment *945*: Common spruce stands planted in 1918 and exploited in 2012.
- Compartment *950*: Common spruce stands planted in 1918 and exploited in 2016.
- Compartment *955*: Common spruce stands planted in 1914 and 1930 and exploited in 2008.

These three compartments are delimited by two paths. These correspond to the three main areas within our study site that are illustrated in Figure 9 and 10.

There has been a change of vocation in the area during the years 2017 and 2018. The area went from a "Forestry" vocation to a "Nature Conservation" vocation. The numbers of the compartments have thus changed, *945* became *422* whereas the previous compartments *950*, *951*, *955*, *956* and *963* form the new compartment *438* represented in the following Figure 13.

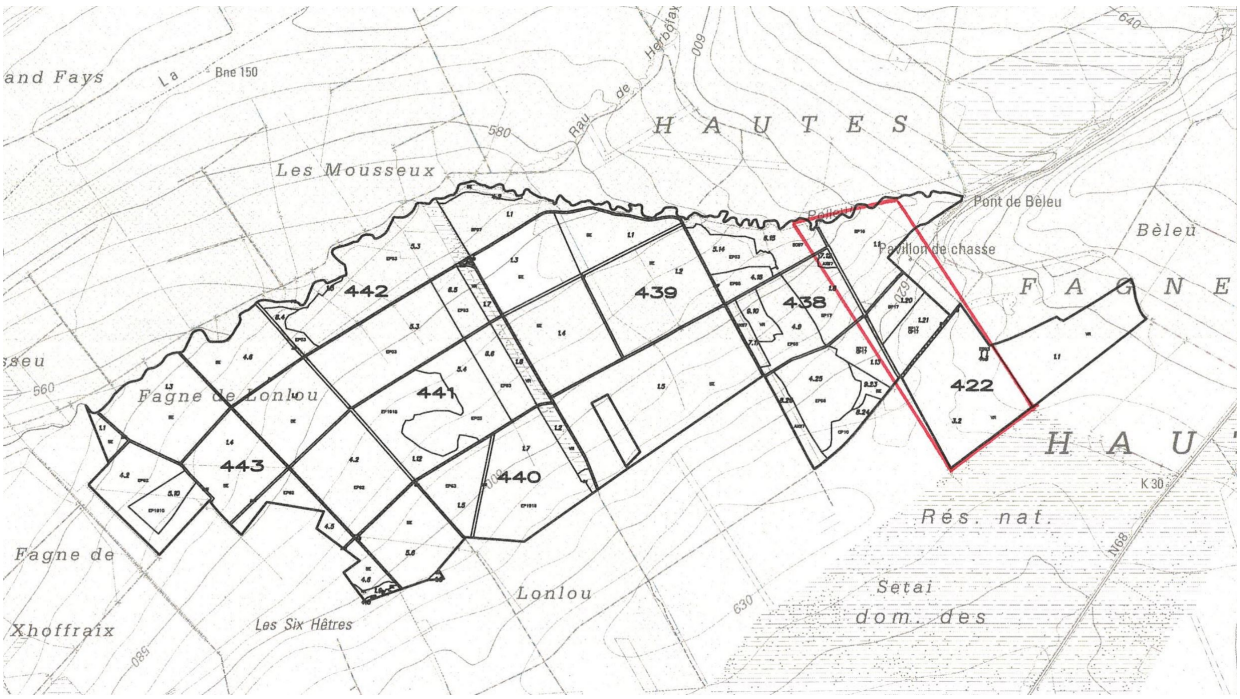

Figure 13: Present distribution of the compartments of the High-Fens State Nature Reserve [10]

New populations were planted during the years 2016 to 2017, after the clearing of the area a few years earlier. These are represented in Figure 14. Downy birch (*Betula pubescens*) are predominant on most of the site, as they were planted on light green and pink areas. Pedunculate oak (*Quercus robur*) were also planted on light green areas as well as the yellow area on the plateau. To a lesser extent, common alder (*Alnus glutinosa*) in the red area, as well as a few remaining common spruce (*Epicea abies*) in the dark green areas. Spruce stands were not fit for peaty soils. These compartments now recently converted to the state nature reserve of the High Fens, only essences adapted to the soil will be planted, in the hope of bringing back the natural habitats of the past. Most deciduous trees that will be planted are the majority of the previously mentioned in Figure 14: Downy birch as well as pedunculate oak, both being adapted to peaty soils.

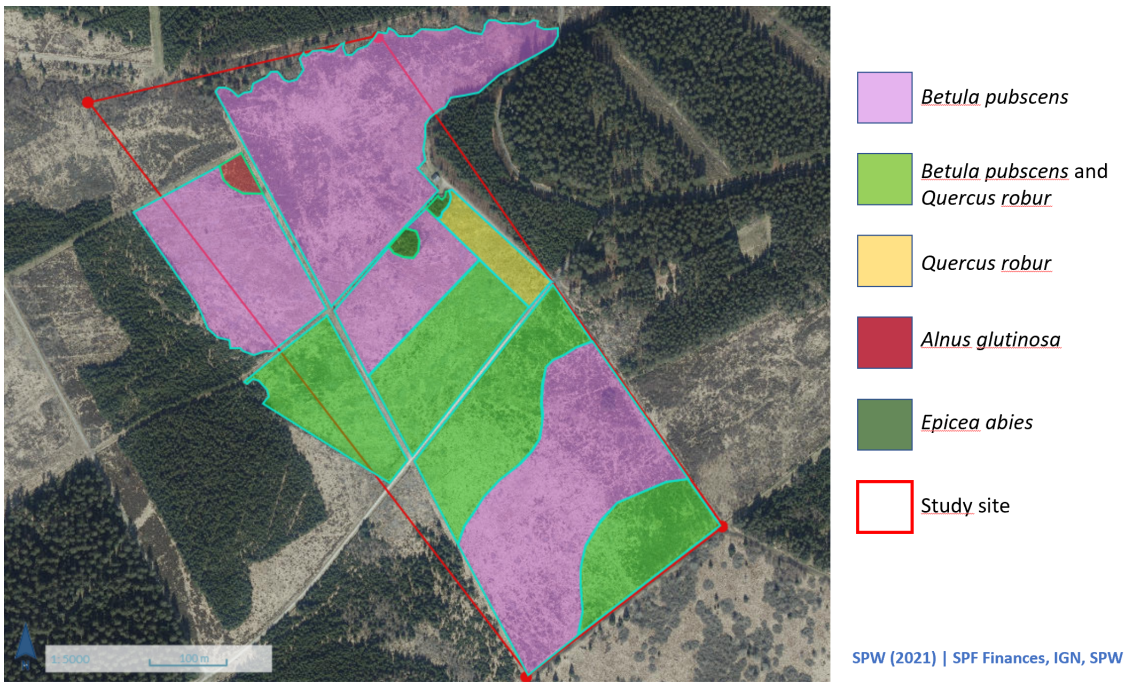

Figure 14: Deciduous trees plantation during the years 2016 to 2018 [10]

It appears clearly on the orthophoto shown in Figure 9 and in Figure 15, that the trees on site were recently cut down, as the vegetation is limited to a few adult birch trees left for local sowing of the contiguous compartments as well as a few remaining common spruce represented by the dark green areas from Figure 14. As previously mentioned, there are areas with young trees surrounded by protective metallic fences, as well as unprotected young tree shoots. However, the vast majority of the area is covered by numerous clusters of *Molinia caerulea*, as can be seen in Figure 15.

Figure 15: Picture taken by Pr. Lambot Sébastien on February 9^{th} on the bottom of the slope, at the northern edge of the study site

5 Methodology

5.1 Hydrogeophysical methods

Traditional study methods of the environment essentially rely on destructive data acquisition or are based on interpolation between punctual measurements. This proved to be a problem when it comes to assessing some spatially varying characteristics of a study site on the field-scale. Another type of approach based on technological advances aims to overcome the drawbacks of these traditional methods. In recent years, non-invasive geophysical and remote sensing methods have provided new opportunities for measurements and imaging of field characteristics. Multiple forms exist, such as electromagnetic induction (see Section 5.2), electrical resistivity tomography, ground-penetrating radar (see Section 5.4), etc. Sensor networks such as soil moisture monitoring and temperature monitoring are new techniques that allow for a better tracking of field conditions evolution through time [61]. The potential for application of geophysical methods is vast, an important part of what we know about the Earth comes from indirect observations such as variations in gravity, magnetic, electric and electromagnetic fields, etc. The opportunities keep expanding as computing and electronic technologies further develop [62].

Hydrogeophysics is a specific research domain that applies geophysical methods to provide quantitative information about hydrogeological parameters and processes. It benefits from the experience of geophysical techniques that have been used by the mining and petroleum industries for over 50 years and applies them to purely hydrology-related objectives such as estimating subsurface water resources, contaminant transport as well as ecological and climate investigations [63].

5.2 Electromagnetic induction

5.2.1 Principles

EMI instruments allow for non-invasive subsurface characterization. These types of measurements have a lot of potential for multiple reasons. In addition to being relatively low cost, EMI presents the advantages of being easy to use, mobile, fast and capable of gathering important volumes of data. This makes it ideal for performing quick measurements on relatively large areas [61, 64, 65].

EMI instruments emit magnetic waves at low frequencies (below 10^5 Hz). The primary magnetic field (H_P) is generated by an electrical current passing through the transmitter coil (Tx). This primary field H_P induces eddy current in electrical conductive subsurface through induction phenomena. The eddy current generates, in turn, secondary magnetic fields H_S that can be measured by the instrument. The ratio between H_S and H_P can be related to the ground electrical properties [61, 64].

The main characteristic measured by this technique is soil bulk electrical conductivity. However, electrical conductivity readings are a composite of soil properties such as texture (mostly clay content as it is more conductive than loam or sand), water content, temperature, salinity, CEC, pH, organic matter content, nutrients, $CaCO_3$ content, structure, density and finally magnetic susceptibility. The interactions between all these soil properties are complex and may vary over short distances. It is for this reason that EMI data are better interpreted when combined and compared with other study methods [61, 64, 65].

5.2.2 Applications

EMI is widely used to determine the spatial variability of soils on a field scale since the 1970s. It was initially used to map soil salinity and has since expanded to multiple other uses such as soil types mapping, water content assessment, water flow patterns, soil texture variations, compaction, organic matter content, pH and subsurface stratigraphy [65]. Before the emergence of the GPS technology, grids had to be established for each EMI survey. It was only by the mid- to late-1990s, that GPS technology was integrated with EMI sensors, making rapid collection of geo-referenced EMI data possible. This marked a turning point, as it made intensive field-scale surveys practical and commonplace.

The electrical conductivity measurements provided by EMI studies can be used in different fields of research, such as agricultural studies. Electrical conductivity is one of the properties that is correlated to crop productivity, it may also be used to analyze soil nitrogen content or other nutrient content to optimize fertilization or irrigation [64]. These properties make it a good fit for precision agriculture, as well as providing a better understanding of soil-water-plant interactions [66].

EMI studies can also be applied to soil science, where it has already been proved to be a valuable tool to identify soil patterns. It can be used to determine the soil clay content, as well as organic matter content and water holding capacity [67, 68, 69]. Other domains of use exist, such as determining the thickness of sea ice or archeology [64].

5.2.3 Material and methods

The sensor used is an EM38-MK2 by Geonics Limited. This tool provides simultaneous measurements of ground conductivity and magnetic susceptibility. It is equipped with two transmitter receiver coil separations of 1 m and 0,5 m. These two spacings, combined with two dipole modes, allow measuring at 1,5 m and 0,75 m depth for vertical dipole mode and 0,75 m and 0,38 m in horizontal dipole mode. Its operating frequency is 14,5 kHz, it has a conductivity range from 0 to 1000 mS/m, makes 5 measurements every second and can be operated under temperatures ranging between -40°C and 50°C.

In this study, the chosen coil spacing was 1 m and the vertical dipole configuration was used. The device was equipped with straps and carried by hand, as close to the ground surface as possible. The measurement method is represented in Figure 16. The person carrying the device

had to carry as little conductive materials as possible, as not to cause any interferences with the measured data. The EM38-MK2 was connected by Bluetooth to a computer carried by a second person walking a few meters behind, so not to interfere with the magnetic waves. A portable GPS was also fixated on the EMI and plugged to the computer, receiving the measurements through a cable.

Figure 16: EMI measurement realized on February 9^{th} 2022. Picture taken by Pr. Lambot Sébastien

The measurements were usually made in each of the three areas described in Figure 9, in the form of transects following the topography gradient. The transects were usually followed by at least one return trip, at a distance between 5 m and 10 m from the first one. The data was gathered in the form of a CSV file, each line compiling the information of one measurement such as the time of the measurement, its coordinates, the altitude (although not very precise) as well as the measured ground electrical conductivity and magnetic susceptibility, both for 0,5 m and 1,0 m intercoil spacing. The outliers of each data set were removed by excluding all values inferior to the mean value subtracted by 3 times the standard deviation, as well as the values superior to the addition of the mean value and the triple of the standard deviation. Most removed values seemed to be high electrical conductivity, probably influenced by exterior objects such as metallic fences or metallic equipment encountered at the end of some transect. The data was the imported to ArcGis Pro, where the kriging tool was used to produce the soil bulk electrical conductivity maps displayed in Section 6.1.

5.3 Conductivity probe

5.3.1 Principle

The use of conductivity probes has been deemed coherent for a better interpretation of the EMI results. A conductivity probe is an instrument composed of two main parts: the conductivity cell that makes the measurements, and the conductivity meter that reads and displays the data. The measurements consist of digging a borehole deep enough to reach the water table. The conductivity cell is then lowered in the soil solution to measure its electrical conductivity.

5.3.2 Material and methods

The conductivity meter used during this study is the WTW portable conductivity meter ProfiLine Cond3310. Its advantages are its battery life, its integrated timer for more accurate measurements, as well as its automatic temperature compensation while making measurements. The used conductivity measuring cell is the WTW TetraCon 325, which is adapted to on-site measurements in surface water, groundwater, fish farming, sewage and is also useful in the context of lab analysis.

In the case of this study, the objective of measuring the electrical conductivity of the soil solution is to be compared with the bulk electrical conductivity measured with the EMI, in the hope of strengthening the quality of the interpretation.

A total of 20 holes were dug to measure the soil solution electrical conductivity. The height of the water table was very variable, not allowing us to reach the water table each time. We however still had a minimum of 4 measurements for each of the three areas of the site. The results of these measurements are displayed in Section 6.2.

5.4 Ground penetrating radar

5.4.1 Principle

GPR is a method that uses the propagation of electromagnetic waves below the ground surface to determine the position of buried structures and objects. It is based on the fact that heterogeneities in the electromagnetic properties of the different layers below the surface cause reflection, refraction and transmission of the signal. Just like the EMI technology previously described in Section 5.2, it consists of a transmitter antenna (Tx) and a receiver antenna (Rx). The echoes are picked up by the receiving antenna. The time it takes for the wave to come back to the surface gives information about the object depth in the ground [61, 64].

Most GPR systems use a center frequency between 10 MHz and 3.6 GHz. The attenuation of the wave is due to electrical and scattering losses. There is a compromise between resolution and penetration depth: higher frequencies have higher resolution but low penetration depth, whereas lower frequencies allow for a deeper study at the cost of lower resolution [61].

A radar image can be constructed on the basis of the voltage variations shown in the incoming signal. Indeed, electromagnetic contrasts in the subsurface cause a part of the signal to be reflected, which is observed by a peak, followed by a dip in the voltage [64]. These fluctuations can be represented in the form of an image, such as the ones that will be presented in Section 6.4.

5.4.2 Soil electromagnetic properties

This propagation of the electromagnetic wave is mathematically described by Maxwell's equations [64, 61]. The velocity of the wave in the medium is directly correlated with the relative dielectric permittivity of the medium (ϵ_r), whereas the attenuation of the signal is affected by its electrical conductivity (σ) [64, 61]. The relative dielectric permittivity of pure water (ϵ_r = 80 at 20°C) being way higher than that of air (ϵ_r = 1) and soil minerals (ϵ_r = 3-5), this characteristic alone can provide useful information about water content in the CZ [61]. In some cases, magnetic permeability has to be taken into account, it is however less common. The magnetic permeability of free space is often used ($\mu_0 = 4\ \pi\ \cdot 10^{-7}$ H/m) [64, 61].

5.4.3 Material and methods

Several configurations of GPR can be applied. We will go into more details on two of them in the frame of this master thesis: surface and off-ground GPR.

The **surface GPR** used in this project is shown in Figure 17 is composed of 5 main components. First, we have two bow-tie antennas with a transmitter and a receiver. Both antennas are placed next to each other in the same box. The box containing both antennas is free to move up and down following the topography, thus assuring an optimal contact surface with the soil, which is crucial in order to see deep below the surface. The antenna has a center frequency of 400 MHz, with a lower frequency of approximately 100 MHz and a maximum frequency of about 900 MHz. The other components are a radar system, a main battery, a positioning wheel that acts like an odometer and finally a controlling computer. All these components are mounted on a wheeled frame that is pushed by hand [64]. In the context of this study, the surface GPR allowed to make an image to a depth of 2,2 m below the surface. The results of these measurements are displayed in Section 6.4. GPR measurements have usually a unit: it is V/m however, the color scale used for the GPR profiles displayed in Section 6.4 has no unit since the signal has been transformed multiple times by the use of gain functions. The used color scale is thus relative and highlights electromagnetic contrasts.

Figure 17: GPR system used during the measurements from June 1^{st} 2022. Picture taken by Pr. Lambot Sébastien

The **off-ground configuration** of the GPR is based on the same principle as the on-ground GPR. It has some advantages as well as disadvantages compared to the configuration described previously. Its main advantage is the speed at which data can be collected, as well as the fact that it can make measurements on areas that are much harder to work on with surface GPR because of terrain roughness and vegetation, for example. This makes this method particularly adapted for field-scale measurements at high spatial resolution [61]. The main drawback of the method is the fact that the penetration depth of this method is less than for surface GPR [61]. It is also sensitive to surface roughness, although this can be accounted for during the inversion of the data by using the roughness model proposed by Jonard et al. [70].

5.4.4 Applications

The first recorded attempt at measuring the subsurface dates from 1956, where it was attempted to image the water table depth by using the interferences between air transmitted signal and reflected signals from the water table. In 1961, radio waves were used for the first time to penetrate the subsurface of an ice sheet in Greenland. The technology kept being improved on during the following years, it was even used on the Apollo 17 mission to assess the electrical properties of the surface of the moon from orbit [71].

GPR can be used in hydrogeophysical investigations to determine the geological structure of the subsurface of the soil as well as material properties. It can be used to delineate fine-scale depositional stratigraphy, which partially dictates the groundwater flow. It can also be used for mapping underwater flows as well as the water table [63, 72]. It is heavily used in archeology, civil engineering, mining industry, security, etc. [63, 71, 72].

GPR can also be mounted on drones, as described by Wu et al. [73, 74]. This has been described in the previous Section 5.4.3. This technique has been reviewed and described as being promising, as well as having a good correlation with results obtained by EMI studies [74, 73].

5.5 Soil profiling

5.5.1 Principle

Soil profiling is a pedological manipulation that consists in the excavation of a soil column over a certain depth while minimizing the destructuration of the sample. This technique allows observation of the different soil horizon successions, giving useful insight about the pedology of the study site.

The main interest of this kind of measurement in the context of this study is that it makes it possible to compare the soil profiles with the GPR imagery, in order to read them in the best possible way.

5.5.2 Material and methods

Multiple techniques exist to extract soil profiles, ranging from spade to excavator holes. These different techniques present drawbacks and should be chosen accordingly to the objective of the study. For example, the use of the spade does not allow for a very deep analysis, whereas the use of an excavator presents a lot of more complexity [11].

The material used during this study is a hand auger. This tool is composed of a 20 cm head designed to dig and extract 20 cm of soil, attached to a vertical axis of 80 cm with a horizontal handle on top to rotate the auger. This method proved to be the best tradeoff as the 20 cm head enables an easy preservation of the soil structure with relative ease and allowed for soil profiling of a maximum depth of 1 m.

The soil profiles were done on August 3^{rd} 2022 with the use of a hand auger, a knife and a PVC channel as support for the successive depositions of the auger head content. 10 profiles were reconstructed in total, following the transect of the GPR measurements. Some occasional obstacles prevented us from realizing the full soil profile. 20 cm of soil from the auger head was extracted from the head with the help of a knife and deposited one next to the other. The succession of digging allowed to reconstruct the soil profile in the PVC channel. The profiles as well as their location on the field are displayed in Section 6.3.

6 Results

6.1 EMI

The maps from Figure 18 show the electrical conductivity values measured on the three first measurement campaigns conducted on February 9^{th}, March 8^{th} and March 28^{th}, respectively. The EM38-MK2 sensor measures simultaneously electrical conductivity and magnetic susceptibility. However, the measurements of the latter did not bring much interest, as there does not seem to be any magnetic materials in the soil. Hence, the choice was made of to exclusively focus on the electrical conductivity results.

We made measurements using the vertical dipole configuration for both intercoil spacing (0,5 m and 1 m) to gather data on depths of 0,75 m and 1,5 m, respectively. However, the terrain and the vegetation did not allow for a stable height of the EMI, which noticeably affected the measurements at 0,75 m depth. The important noise makes these measurements unfit for interpretation. The 1,5 m depth measurements are however, less sensitive to height changes of the EMI and present minor disturbances. These measurements will be displayed in Figures 18 and 19.

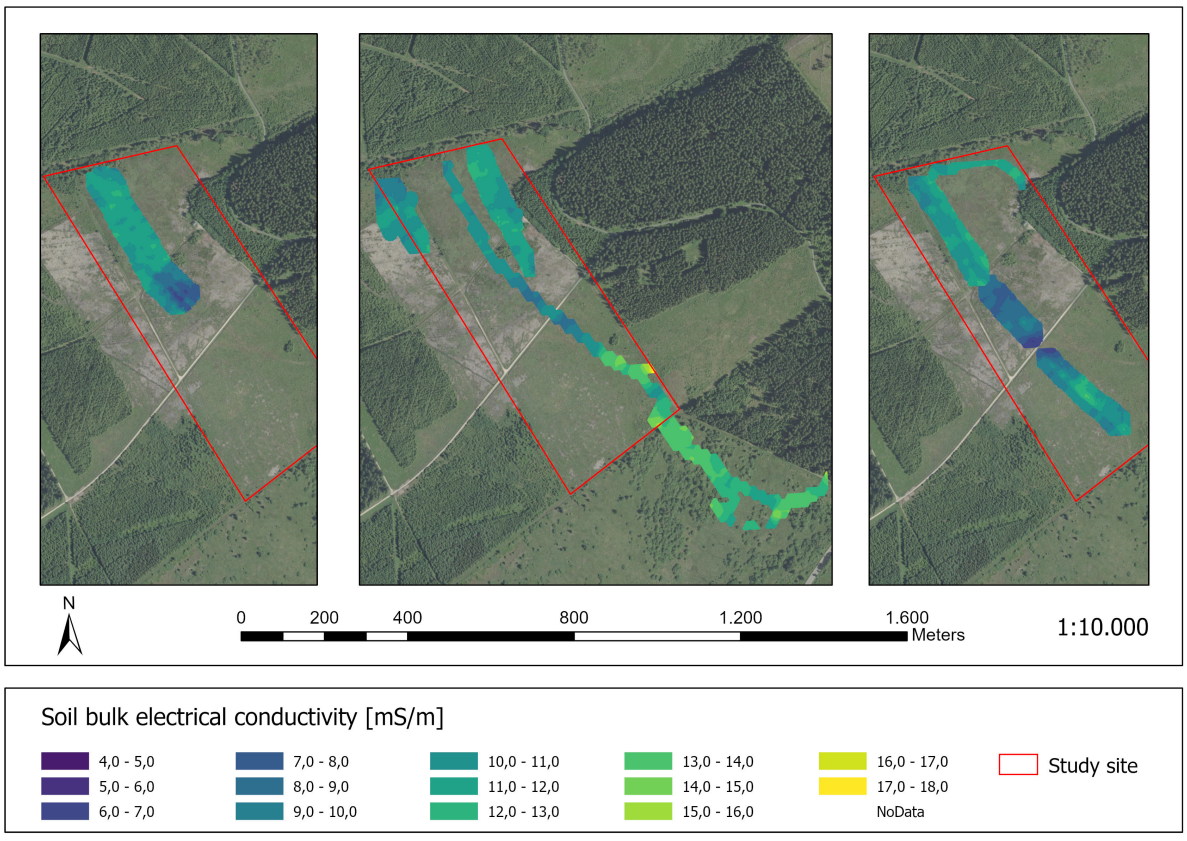

Figure 18: From left to right, soil bulk electrical conductivity measured by electromagnetic induction on February 9^{th}, March 8^{th} and March 28^{th} 2022, respectively.

All three measurement campaigns were conducted under similar conditions, with dry weather and no rain during the 24 previous hours. The soil was also mostly saturated during all three

measurement campaigns represented in Figure 18.

The goal of the February 9^{th} measurement campaign was to assess the variability of the soil electrical conductivity following the topography gradient by comparing results from the slope with measurements from the central plateau (as shown in Figure 10). We can already see a clear contrast between the slope conductivity values, which range between 10,0 mS/m and 13,0 mS/m and the central plateau conductivity values, which range from 5,0 to 11 mS/m, on the south-west. Both areas have fairly consistent bulk electrical conductivities, with the central plateau showing much lower values than on the slope, except on the south-west where it is higher.

The second transect was done with the intent of covering a much larger distance to see if there is any variability on a larger scale, even outside the study site boundaries. The goal was also to cover different soil types, in opposition to the February 9^{th} campaign, which was exclusively done on "peat soils or bogs" according to the soil types map of WalOnMap shown in Figure 11. We also made measurements on two small areas on the east and west to see if these zones could prove to be of particular interest for future studies because of the different types of soil seen on the pedology map. The measurements on the slope are fairly homogeneous, with comparable values than on February 9^{th}. The plateau has higher bulk conductivity compared to the first campaign, but is still globally lower than in the slope (range between 8,0 and 10,0 mS/m). Just across the road, the southern plateau presents low values, comparable to the ones measured on the central plateau, and seems to have overall higher bulk conductivity, ranging from 8,0 to 15 mS/m, the higher values being caused by interferences with the metallic fence. The conductivity measured outside the study site is overall the highest of the whole transect, with values between 12,0 and 15,0 mS/m.

The two first campaigns allowed for a better understanding of the terrain, based on which we settled the final area to map. The original intent was to follow the topography gradient in the best possible way. However, as can be seen in Figure 18, we did not exactly follow the topography gradient represented in Figure 10 as the altitude gradient goes towards the south-east. This choice was made considering several parameters. Starting from the south-eastern corner would prove difficult as it is densely populated with small birch trees (see Figures 9, 14) as well as bramble, which made the navigation in this part of the site difficult. We ended up with the third transect represented in Figure 18 as it followed the topography fairly well and would allow for a much easier gathering of data, we also followed the river along the northern boundary of the study site. The measured bulk conductivities are similar to the ones from February 9^{th} and March 8^{th}, with conductivity values even dropping around 4,0 mS/m on both sides of the main road (in the central and southern plateau). The path followed on the southern plateau was not exactly the same as on March 8^{th}, but the lowest value on the northern limit of the area is consistent. The rest of the southern plateau is usually around 11,0 or 12,0 mS/m, with a slightly lighter spot in the middle of around 14,0 mS/m.

A last EMI measurement campaign was realized on June 24^{th} 2022 (Figure 19), following the same path as for the March 28^{th} campaign represented in Figure 18. This campaign was done three months later than the previous one. The objective was to observe any potential changes

in the bulk electrical conductivity of the soil under different soil moisture conditions. It did not seem to be the case, as the electrical conductivity values we measured were similar to those previously measured in February and March. The only notable difference between the June measurements and the other ones being the conductivity on the plateau, in the middle of the transect. These are much more homogeneous with the rest of the values measured along the transect, compared with the three first measurement campaigns, with measured conductivities from the slope and the central plateau ranging between 10,0 and 12,0 mS/m. The lighter spot in the southern plateau visible on the March 18^{th} measurements is much more visible, reaching an electrical conductivity of 16,0 mS/m.

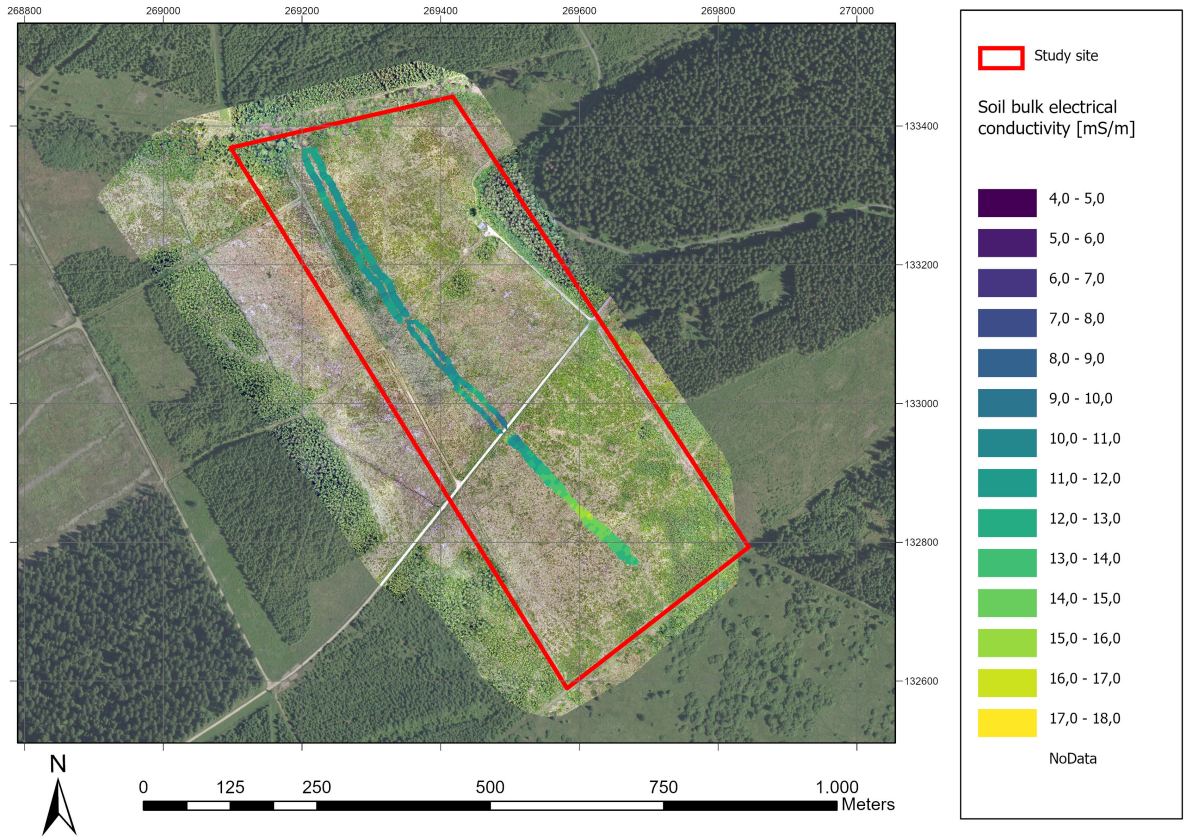

Figure 19: Soil bulk electrical conductivity measured on June 24^{th} 2022

6.2 Conductivity probes

Measurements of the soil solution electrical conductivity were realized on June 1^{st} 2022 along the final transect followed with the EMI on March 28^{th} and June 24^{th}. The objective was to determine the influence of the liquid phase on the bulk conductivity measured by EMI. The results are displayed in Figure 20. The bulk electrical conductivity of the study site represented in Figure 20 is from June 1^{st} and was measured three weeks after the soil solution conductivity. We chose to compare the soil water conductivity with the temporally closest bulk conductivity measurements.

The role of the map represented in Figure 20 is to compare the soil water conductivity with

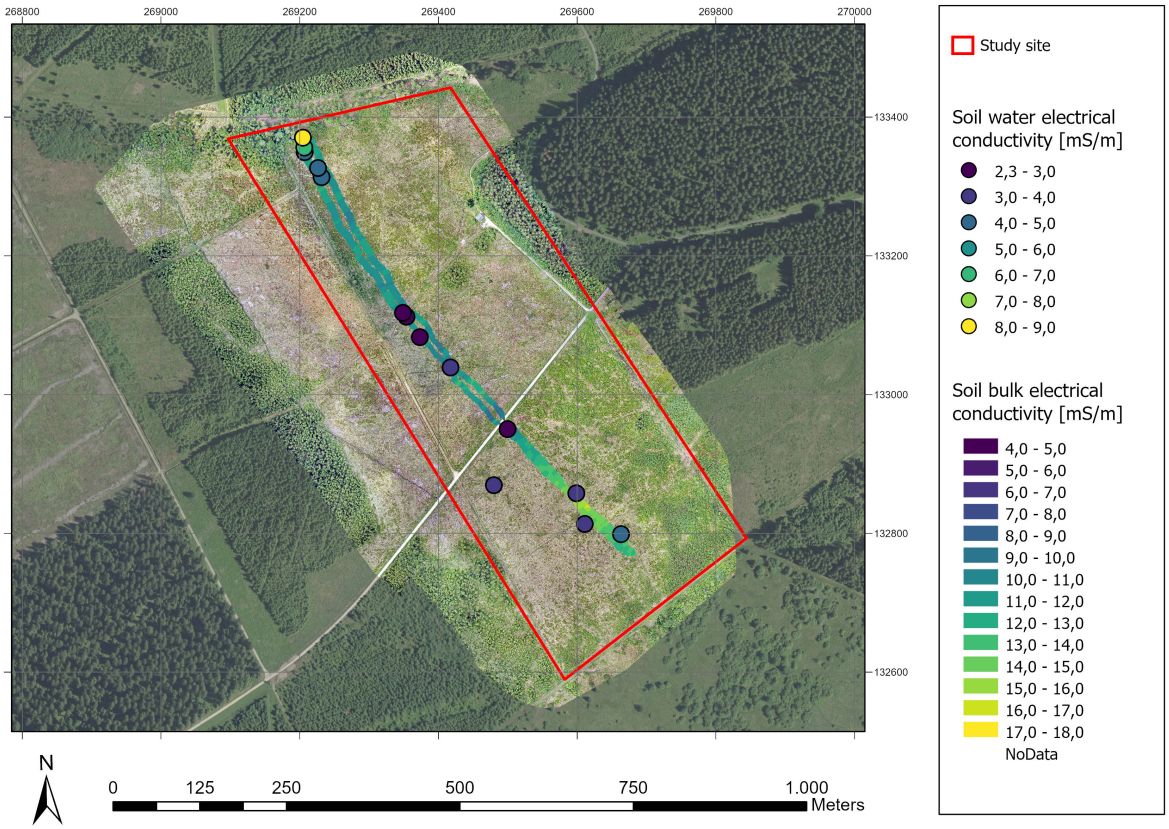

Figure 20: Soil water electrical conductivity measured on June 1^{st} compared with the bulk conductivity of the soil measured on June 24^{th}

the bulk electrical conductivity. The measured soil water values are a combination of surface water and groundwater measurements. As the value ranges are similar for both surface and groundwater, both are represented on the above map with no distinction, for more clarity.

We can observe that the conductivity of the water phase is lower than that of the bulk conductivity, the latter does not drop below 7,0 mS/m. The highest measured water conductivity comes directly from the river Polleur, on the northern limit of our site, and reaches 8,0 mS/m. As for soil water conductivity, the highest measurement comes from a sampling right next to the river, with a value of 6,6 mS/m. All the other values range from 2,3 mS/m to 4,5 mS/m. Interestingly, the lowest measured value comes from the drain at the top of the slope. We can observe that all samplings realized at the bottom of the slope have overall higher conductivities than the ones on the central and southern plateau. These observations are best explained by the fact that the solutes may have been transported downhill by water, leading to their accumulation at the bottom of the slope and increasing the soil solution conductivity.

6.3 Soil profiles

To strengthen the interpretation of the GPR data from June 1^{st} 2022 (see Section 6.4), a series of soil profiles was realized on August 3^{rd} 2022. The most interesting profiles will be presented in this Section and will later be discussed and compared to the GPR imagery presented in

Section 6.4. The locations of the 10 soil profiles made along the GPR transects are labeled in white in Figure 21. In the following map, the soil profiling points are superposed to the GPR transects to better interpret the GPR imagery. The whole length of the GPR transect was subdivided into 10 smaller ones and are labeled with black numbers in Figure 21. This decision was made for multiple reasons. First, this was done in order to divide the whole GPR profile into smaller ones to have images of reasonable size. The second reason is that the GPS and GPR data were collected separately. The GPS data was not as precise as for the EMI measurements.

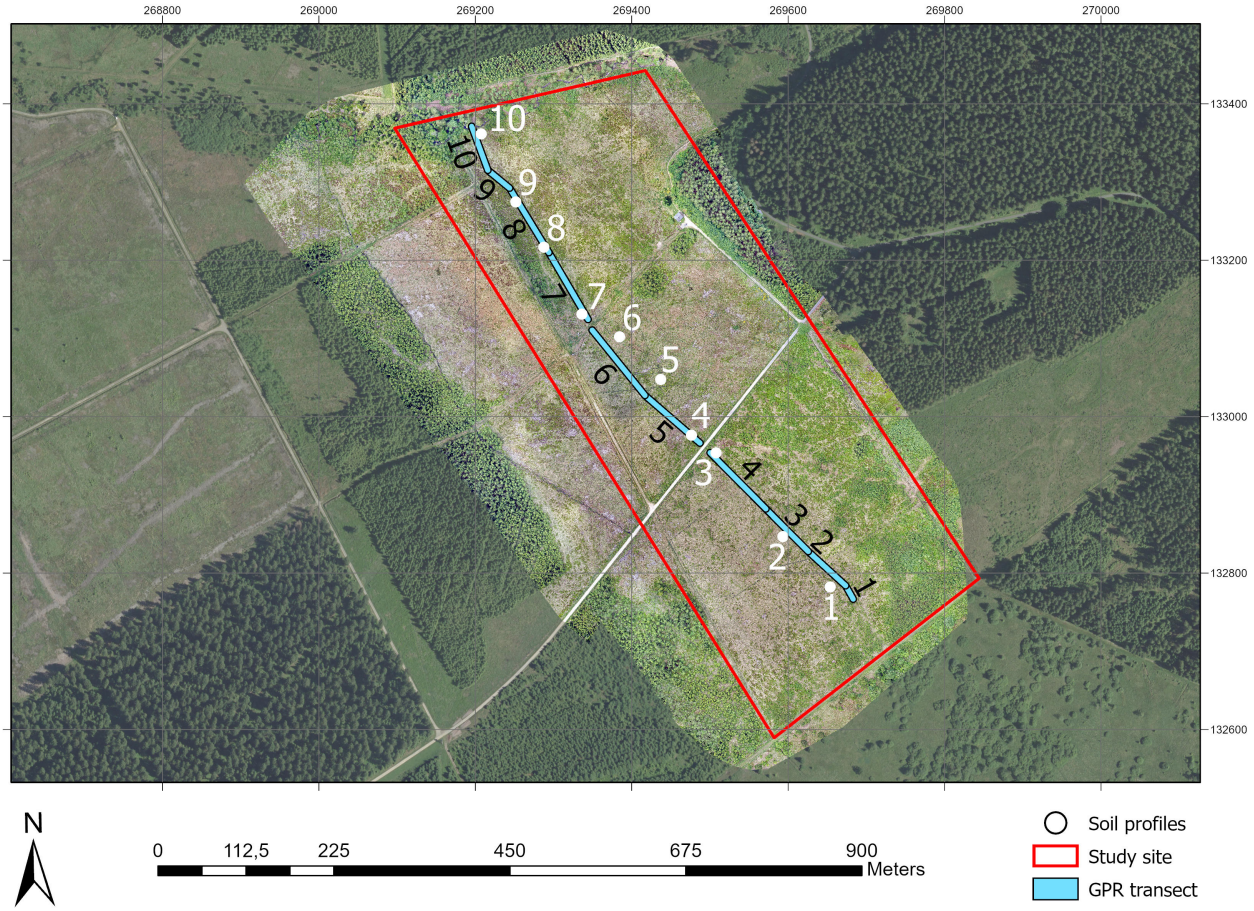

Figure 21: In white are represented the locations of the 10 soil profiles realized on August 3^{rd} and in black are numbered the 10 GPR segments previously presented

Figure 22 displays two soil profiles from the southern plateau from the GPR transects 3 and 4 (displayed in Figures 6.4.1 and 6.4.2). Figure 23 displays two soil profiles from the central plateau on GPR transect number 5 presented in Figure 6.4.3 and one profile from the top of the slope (transect 7, presented in Figure 28). These multiple profiles will be a tool for the interpretation of the subsurface imagery from Section 6.4.

(a) Soil profile 2 (b) Soil profile 3

Figure 22: Soil profiling realized on the southern plateau of the study site on August 3^{rd} 2022

(a) Soil profile 4 (b) Soil profile 5 (c) Soil profile 7

Figure 23: Soil profiles realized on the central plateau and slope of the study site on August 3^{rd} 2022

Profile 2 is visible in Figure 22a and shows roots on the first 15 cm, followed by dark and humid peat containing wood fragments. There is a transition to blueish-gray clay between 60 and 80 cm and finally pure clay on the end of the profile.

Profile 3 displayed in Figure 22b is fairly dry and shows the clear presence of roots on the first 10 cm. The upper peat layer shows a transition to loam around 30 cm depth. The profile is only 55 cm deep because a rock prevented us from going deeper.

Profile 4 (Figure 23a) is dry and is located on the central plateau. The peat layer is thin and shows a transition to brown loam between 10 and 15 cm depth. A second transition is observable at 50 cm, where there is a switch to a more clayey loam with a lighter color. A rock at 80 cm depth prevented us from going deeper.

Profile 5 is displayed in Figure 23b. The roots reach a depth of 8 cm and the peat layer is very thick, the first dark peat layer reaching 45 cm depth before transitioning to a more brown peat. This second peat layer transitions to blueish gray clay at 80 cm depth. This profile was particularly wet.

Profile 7 displayed in Figure 23c was done on the heights of the slope with the intention of reaching the peak visible at the 10-meter mark of the GPR image from Figure 28 that will be presented in Section 6.4. Roots extend to the first 10 cm below the surface. The topsoil layer is peat with a fairly low degree of humification, with multiple fibers visible. At 55 cm, there is a transition to a blueish gray layer that seems to be a mix of clay and slate fragments. This suggests that the bedrock of the study site is slate, as it is common in the Stavelot-Venn massif (see Section 4.4).

The other soil profiles either did not show much interest or were consistent with the neighboring ones. These are displayed in the Appendix Section.

6.4 Subsurface GPR imagery

The GPR measurements were realized on June 1^{st} 2022, along with the soil water electrical conductivity measurements. The smaller transects are displayed in Figure 24.

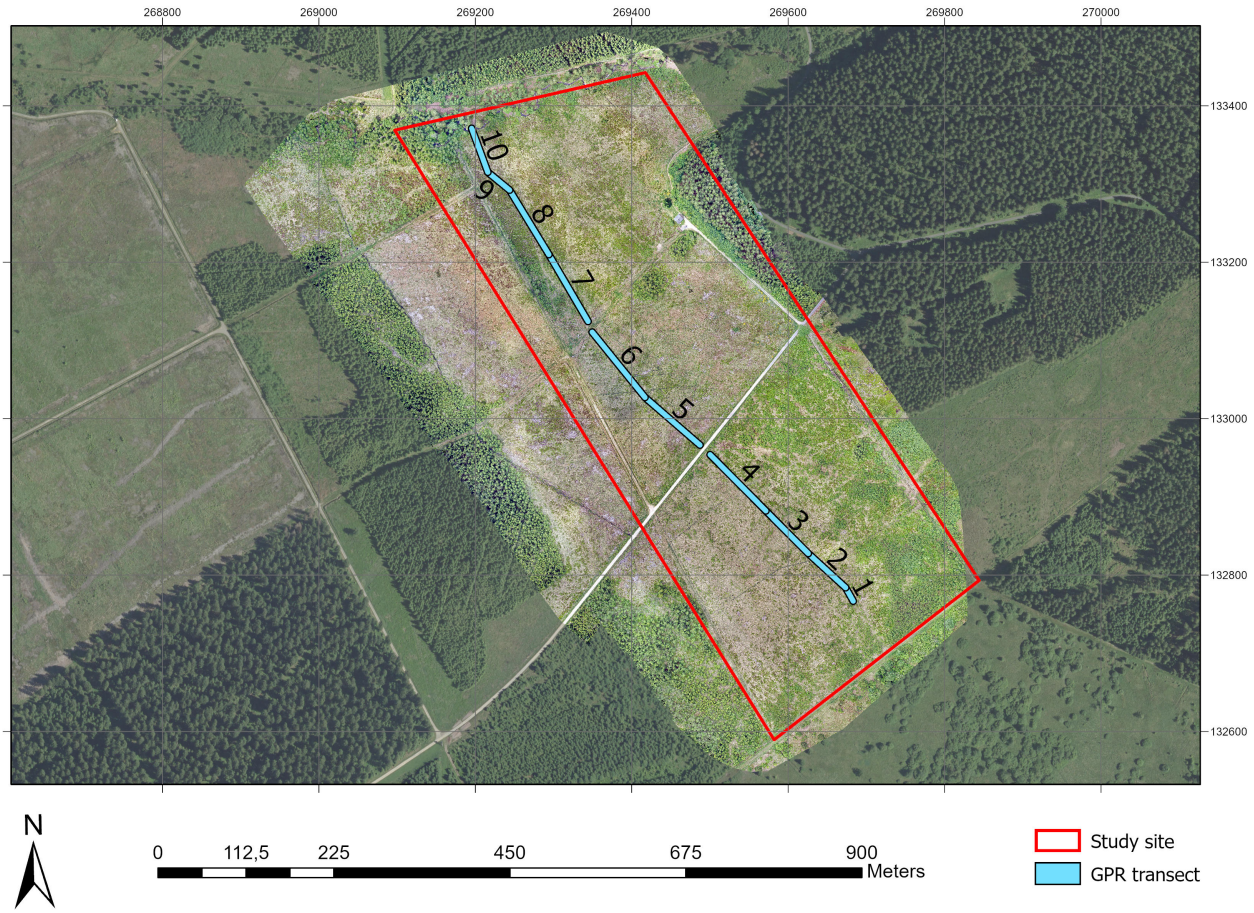

Figure 24: Highlight of the 10 different GPR profiles measured on June 1^{st} 2022

At least one representative transect of each of the three zones delimited in Section 4.1. These will be transects 3, 4, 5 and 7 will be illustrated by Figures 25, 26, 27 and 28, respectively. All profiles are presented in direction south to north.

6.4.1 Subsurface image of GPR transect 3 on the southern plateau

Figure 25 is the transect labelled 3 in the map from Figure 24. This transect has been chosen for deeper analysis because of the higher bulk electrical conductivity observed in Figures 18 and 19. We can distinguish four main layers at 20 cm, 40 cm, 1,2 m and 2,1 m depth. Soil profile 2 (Figure 22a) has been done in the middle of the transect, on the 40-meter mark from Figure 25.

The first observation is that the depths of the layers do not match the ones seen on profile 2. With the observations from the soil profile number 2, we can hypothesize that "Layer 1" is the vegetation. If that this is the case, all layers should appear deeper in the GPR imagery than in reality. This would mean that "Layer 3" at 1,20 m depth would be the clay layer. According to the observations from soil profile 7 (Figure 23c), "Layer 4" is very likely to be the bedrock. "Layer 2" doesn't fit to any of the observations from soil profile 2. This layer may be noise or the water table.

”Layer 1” does not appear as clearly as the other layers throughout the transect. It may be that this first layer is noise and that ”Layer 2” is actually the influence of the vegetation.

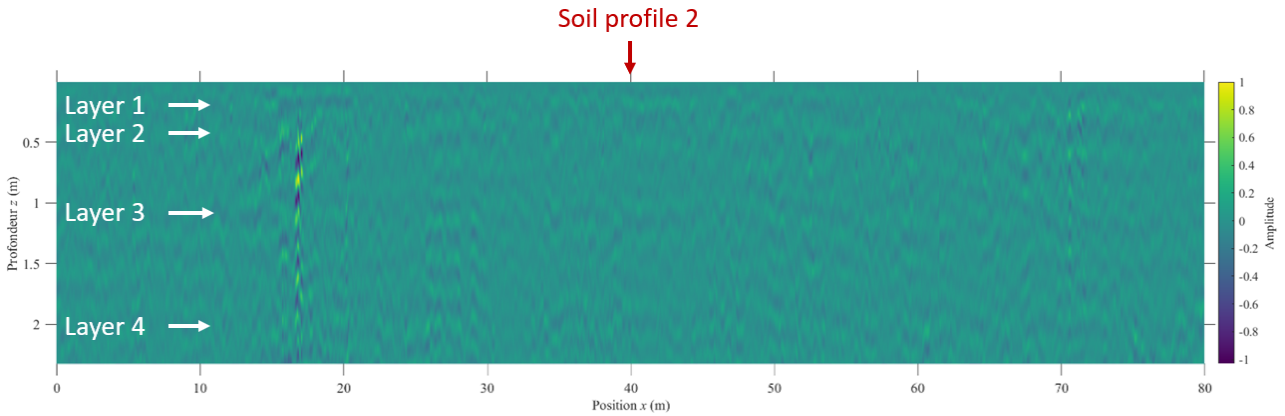

Figure 25: Subsurface image of GPR transect 3 from the GPR transect represented in Figure 24

In this image, all layers seem to be fairly horizontal and are recognizable in all four profiles from the southern plateau. There is an important reflector around 17 meters, and it seems that there is a layer rising from 80 to 50 cm depth right before. This is probably a rock or some other object causing a reflection hyperbole.

6.4.2 Subsurface image of GPR transect 4 in the southern plateau

On the subsurface imagery displayed in Figure 26, we can identify 4 layers, one at 20 cm, 50 cm, 1,20 m and 2 meters depth. Once again, we see a difference between the depths observed in profile 3 (Figure 22b) and the GPR imagery. Soil profiling 4 has been done close to the end of this transect, around the 95-meter mark.

Following the same logic as for the previous transect, ”Layer 1” is the influence of the dense *Molinia caerulea* vegetation. ”Layer 2” has a depth of around 50 cm, this corresponds to the transition from peat to loam from the third soil profile. ”Layer 3” is impossible to identify, as our soil profile only reached a depth of 55 cm. This third layer is located at 1,20 m depth, it is unlikely that this corresponds to the rock that prevented us from digging deeper. ”Layer 3” and ”Layer 4” are located almost exactly at the same depths as in the previous profile. These will thus be interpreted in the same way as being clay and bedrock, respectively.

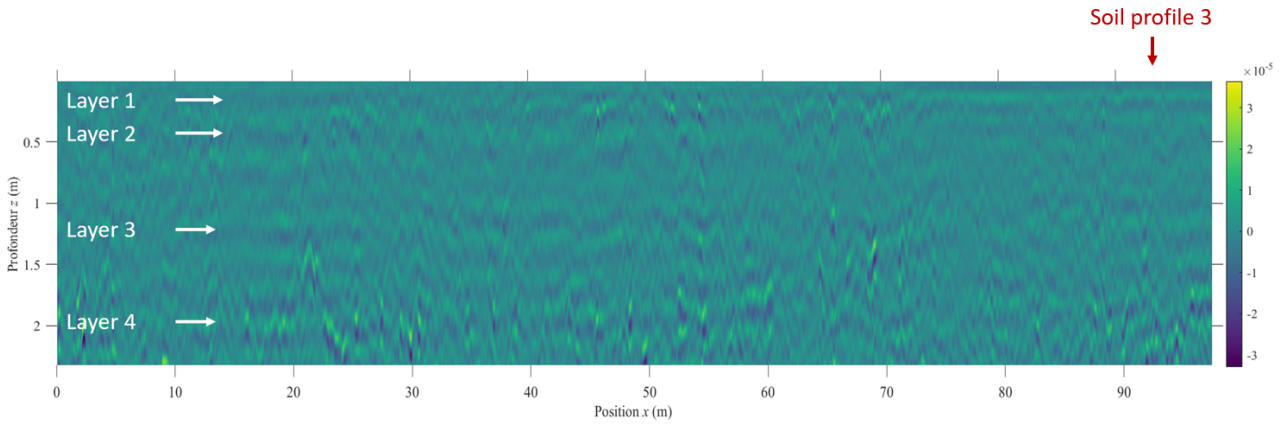

Figure 26: Subsurface image of GPR transect 4 from the GPR transect represented in Figure 24

We can see a slope between 50 m and 80 m along the horizontal axis between the third and fourth layer. One way to see it is that the fourth layer is the bedrock rising towards the surface and stabilizes horizontally at 1 meter depth. Another interpretation is that the third and fourth layers are both bedrock, and that the slope that rises on the second half of the profile is actually a crack in the rock. The water and air present in the crack could explain the observed contrast.

This may also be a soil layer being gradually covered by another one. This may be the loam layer, even though the visibility makes it hard to interpret.

6.4.3 Subsurface image of GPR transect 5 on the plateau

Figure 6.4.3 corresponds to transect number 5 from Figure 24. We can distinguish 4 major layers here, all horizontal at 15 cm, 35 cm, 1,2 m and 2,1 m depth. Soil profile 4 (Figure 23a) is located around the 12-meter mark, and soil profile 5 (Figure 23b) is located at the very end of GPR transect number 5.

When looking at profile 4, ”Layer 1” here corresponds to the root influence. ”Layer 2” corresponds to the peat layer that extends up to 15 cm depth. ”Layer 3” is the transition to clayey loam and ”Layer 4” is bedrock.

However, the structures of soil profiles 4 and 5 differ radically. We should expect to see the top layers get more thick between the start and the end of this GPR image, as the peat layer goes from a thickness of 15 cm to 80 cm. We can observe that on the far right of the GPR imagery, both ”Layer 1” and ”Layer 2” have dropped of around 15 cm, when compared to the beginning of the transect. The first layer is interpreted as being the vegetation influence. The second layer is the transition between the black peat to the brown one (visible on profile 5 in Figure 23b). The third layer is clay and the fourth is bedrock.

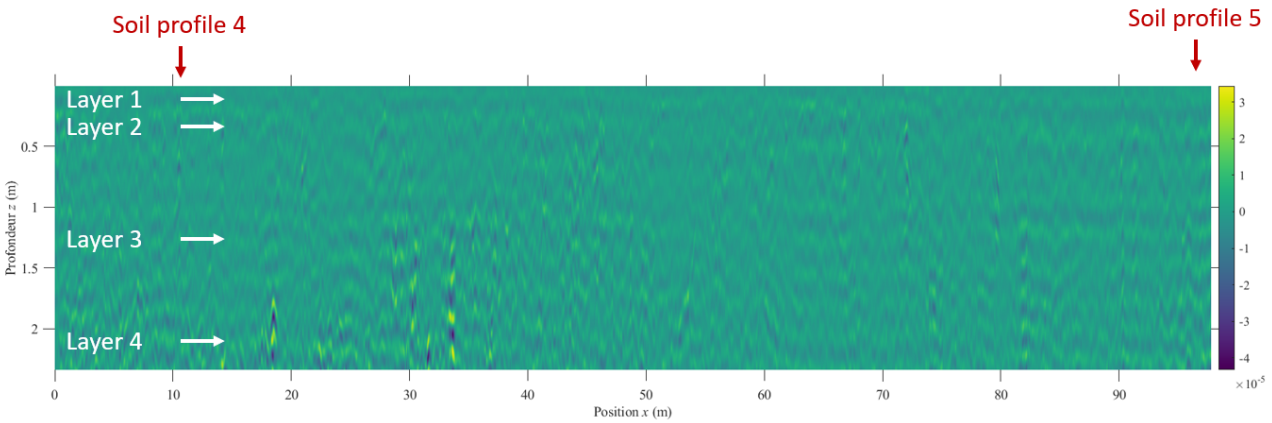

Figure 27: Subsurface image of GPR transect 5 from the GPR transect represented in Figure 24

The dip of the layers in the GPR image is not the same as in the soil profile. This can be explained by the difference in water content. Soil profile 4 was very dry, whereas profile 5 was saturated on August 3^{rd}. If we assume that the water content was similar during the GPR measurement and the soil profiling, that would mean that the electrical permittivity was different for the two soil profiling locations. Different electrical permittivities mean that the electromagnetic signal sent by the GPR would have had different velocities in both locations, explaining the depth difference between the GPR image and soil profiles 4 and 5.

As for the second peat layer present in profile 5 but not profile 4, it may be the 50 cm dip visible at 50 cm depth between the 55 and 60 meter marks. The brown peat layer would have been covered by another one, much darker, around that location.

6.4.4 Subsurface of GPR transect 7 on the slope

Figure 28 is the image of the subsurface at the top of the slope, corresponding to the transect number 7 from Figure 24. The location of soil profile number 7 (Figure 23c) has been chosen after seeing the important peak at the 10 meters mark of Figure 28. Soil profile 7 was done as close as possible to the top of this peak, to better understand this singular observation. On the 10-meter mark, the layers have a depth of 20 cm, 50 cm and 1 m.

"Layer 1" is the influence of the vegetation roots whereas "Layer 2" is clay but with the influence of "Layer 4", which is the slate bedrock. The second layer is less constant than what we have observed on the other GPR images, as it seems to dip and rise multiple times on the second half of the transect. The third layer is very constant over the whole length of the profile. We can see that the bedrock goes steadily towards greater depths after its 10 m peak. It rises again around 43 m before dipping again under the maximum depth of our GPR imagery.

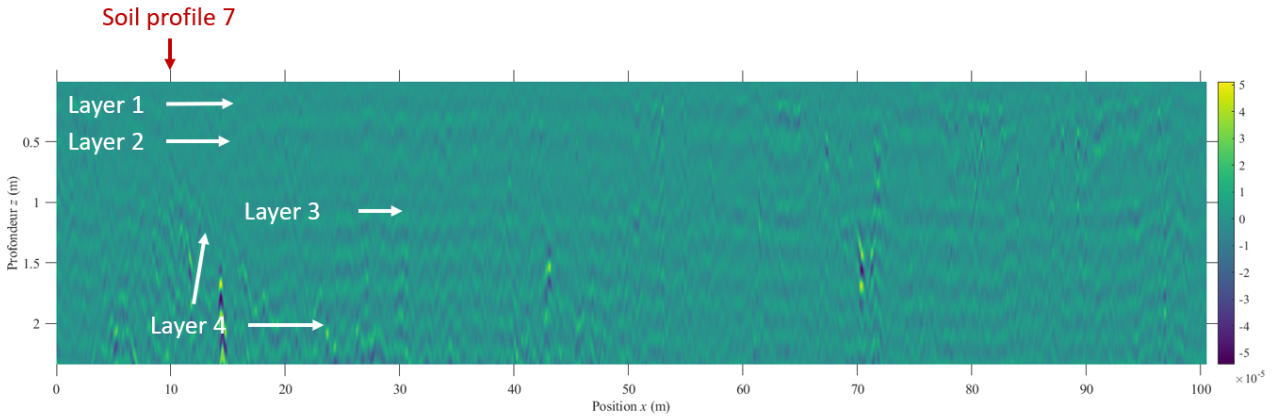

Figure 28: Subsurface image of GPR transect 7 from the GPR transect represented in Figure 24

"Layer 3" is not visible in the location of soil profile 7. The fact that the depth of the layers observed on the GPR imagery differs from reality is because the permittivity value used during the reconstitution of these images was too low. This has had for effect of creating an offset in the estimated depths for all GPR images.

6.5 Low frequency GPR

For this study, the drone flights were realized at an altitude of about 7 meters above the soil surface. The setup used for this study consists of multiple components. First, the frequency-domain radar system, which mainly consisted of a handheld VNA ((Planar R60, Copper Mountain Technologies, Indianapolis, USA. Size: 130 × 65 × 28 mm); a GPS receiver (GlobalSat BU353S4); an Intel R Compute stick, as well as a smartphone-type power bank. The microcomputer is remotely controlled with the use of Python and Javascript programs. A smartphone or tablet is also used and finally, a 5-meter half-wave dipole antenna (VHA 9103, Schwarzbeck Mess-Elektronik, Germany) [73, 74]. The operating frequency is much lower than that of surface GPR, ranging from 15 to 45 MHz, in order to be mostly sensitive to soil electrical conductivity [74].

These results were however, not usable, as the measured electrical conductivity was not consistent with previous EMI measurements. This is likely due to the fact that the estimated permittivity used by the model to get the results was much lower than the actual permittivity of the very wet soil conditions. Another factor that is likely to have affected the results is the fact that the used model assumes a homogeneous half-space, whereas we saw in Section 6.3 that the soil layers of our site can be fairly shallow in some areas.

7 Discussion

Previous studies inform us that field observation of the electrical conductivity of peat soils can be very heterogeneous, ranging from a few mS/m up to over 1 S/m [75, 76]. Schumacker et al. [56] studied the subsurface of the High Fens peatlands in 2002, mostly with GPR technology. They made electrical conductivity measurements and measured values inferior to 10 mS/m in their control sample.

As we can see in Figures 18 and 19, the electrical conductivity measured on our site does not show important variability and is in general fairly low. The values measured during this study are actually comparable to the values measured by Schumacker et al. [56], although being slightly lower. During their 2022 study, Schumacker at al. [56] locally measured values as high as 25 mS/m, but it is important to consider the difference in the methods used. They used in-situ measurement methods, whereas this study focused on EMI measurements, which integrate the conductivity over a certain depth.

The electrical conductivity of soil depends on both the liquid phase such as the fluid saturation, and its concentration in dissolved solids. It is also affected by the solid part of the material, in particular clay content, which strongly increases soil electrical conductivity. Conductivity is also strongly controlled by temperature and affected by other properties of peat like cation exchange capacity (CEC), organic content, structure, heterogeneity, pH and water content.

7.1 Soil electrical conductivity mathematical model

Rhoades' relationship regards bulk soil electrical conductivity σ as being the result of two parallel conductors: a bulk liquid-phase conductivity σ_b associated with the free salts dissolved in the soil solution. The second is the bulk surface conductivity σ_s, associated with the exchangeable ions at the solid/liquid interface.

$$\sigma = \sigma_b + \sigma_s \tag{1}$$

Assuming that the bulk liquid phase conductivity σ_b depends linearly upon the soil water electrical conductivity σ_w and that only the wet fraction of the soil pores conducts currents, we can express Equation (1) as such:

[77, 63].

$$\sigma = \sigma_w \cdot \Theta \cdot T(\Theta) + \sigma_s \tag{2}$$

where Θ is the volumetric water content and T is a transmission coefficient. T accounts for the tortuous nature of the water flow and the decrease in mobility in soil pores

$$T(\Theta) = a \cdot \Theta + b \tag{3}$$

The parameters a and b being soil specific constants. Equation2 shows how the solid phase electrical conductivity is independent of the soil moisture in Rhoade's relationship. It also shows that the importance of the liquid phase in the bulk electrical conductivity is directly correlated with the soil water content.

According to Walter et al. [55], the bulk conductivity of a peat soil is determined by its large porosity (up to 95%) as well as its small bulk density (ρ_b, from 0,05 to 0,5 g cm^{-3}). Samples from our study site have enabled us to calculate the mean density of the peat, which is 0,25 g cm^{-3}. This is a fairly low value that fits in the range described previously. Walter et al. [55] and Comas et al. [75] specifically studied peat soil conductivity. According to both these studies, pore fluid conductivity is proportional to the amount of dissolved ions per volume unit and the surface conductivity is mostly determined by the organic matter content as well as its degradation state [55, 75]. Both studies also concluded that, in the case of peat, σ is mostly determined by σ_w [55, 75]. Walter et al. [55] even got as far as quantifying coefficients linking the relative importance of parameters on σ on a multisite analysis. Pore fluid conductivity σ_w had the strongest effect (x = 0,62), followed by CEC (y = 0,47) and water content Θ (z = 0,11).

The observations were however different for single-site approach. The statistical analysis conducted by Walter et al. [55] indicated that the fluid conductivity σ_w was not the most important contributor to the bulk conductivity σ anymore, contrary to the observations from the multisite approach. This time it was the water content Θ that had the most important influence with a correlation coefficient of z = 0,72. This coefficient is even higher than the one linking σ_w to σ in the multisite analysis approach. This has been interpreted by the fact that the range of σ_w is smaller on a single-site analysis, compared with a multisite analysis.

This model is a useful tool for better understanding the different parameters that influence the bulk electrical conductivity σ of the soil. However, the acquired data does not allow us to realize a quantitative analysis of our data with the help of this model.

7.2 Solid phase electrical conductivity

7.2.1 Humification discussion

A study conducted in 2009 by Bujang et al. [49] concluded that peat soils with higher organic matter content have higher resistivity. This same study also focused on the influence of the humification stage of peat on its electrical conductivity and concluded that the more humified peat is, the higher its conductivity will be [49, 78]. This is due to the fact that the degradation of peat changes its properties on a chemical level by enhancing the formation and release of humic substances and colloidal acids. These represent the most active constituents of peat and have the effect of increasing the CEC as well as the soil physical properties by changing the humus particles quantity, thus affecting the bulk density [49, 55, 78]. As mentioned in Section 7.1, the CEC plays an important part in the bulk electrical conductivity.

The history of our site gives us more insight for the interpretation of the gathered data. As mentioned in Section 4.4, the exploitation of the region in the past has led to intense drainage of the soils from the High Fens. This had the effect of exposing the peat to aerobic conditions, which are favorable to organic matter degradation. On the surface, the peat of the study site seems to have reached relatively high levels of humification. However, the digging of the soil profiles presented in Section 6.3 revealed some fragments of vegetation, especially pieces of wood in some spots.

The bulk electrical conductivity of the soil measured on the central plateau was more homogeneous with the rest of the study in June than during winter, as can be seen by comparing the maps from Figure 18 and 19. We can see that the mean bulk conductivity of the site seems to be around 11,0 mS/m all year long, while the one measured on the central plateau is distinctly lower during the winter, ranging between 6,0 and 8,0 mS/m. This difference is not visible anymore during the June measurements, leading to the assumption that the difference is linked to seasonal changes such as water content.

One heterogeneity that is observable across all EMI measurements campaigns however, is in the southern part of the study site, where the bulk electrical conductivity of the middle of the southern plateau seems to have higher conductivity values than the rest of the site on March 8^{th}, March 28^{th} and June 24^{th}. This heterogeneity doesn't seem to be directly correlated to the humification level, as soil profile 2 (Figure 22a, location shown in Figure 21) contained more vegetation fragments than some other profiles collected in areas with lower electrical conductivity, such as profile 5 (Figure 23b, location shown in Figure 21) for example. This observation goes against the previously discussed effect of humification on electrical conductivity.

The interpretation of the bulk electrical conductivity according to the humification levels of the organic matter of the soil of our study site is inconclusive. Chemical analysis of the peat would however provide a strong tool regarding the importance of this parameter on the soil electrical conductivity.

7.2.2 Pedology discussion

The direct influence of peat and its degradation stages do not have any visible influence on the bulk electrical conductivity of the subsurface. The underlying soil layers may, however, have a more significant impact on the solid phase conductivity on our site. Indeed, with the chosen coil spacing and vertical dipole configuration used for this study, the EMI integrates measured electrical conductivity values over a depth of 1,5 m. If these layers have different electrical conductivities, the fact that their thickness changes along the horizontal axis changes their influence on the measured conductivity.

To assess this hypothesis, we represented the different areas covered during all four EMI campaigns on the main soil types map of Wallonia from the WalOnMap tool of the geoportal of Wallonia [9]. The resulting map is displayed below in Figure 29. As can be seen on the below map, the large majority of the soils covered during the EMI measurement campaigns were classified as "peat soils or bogs" as well as "stony loam soils with mainly moderate to poor natural

drainage".

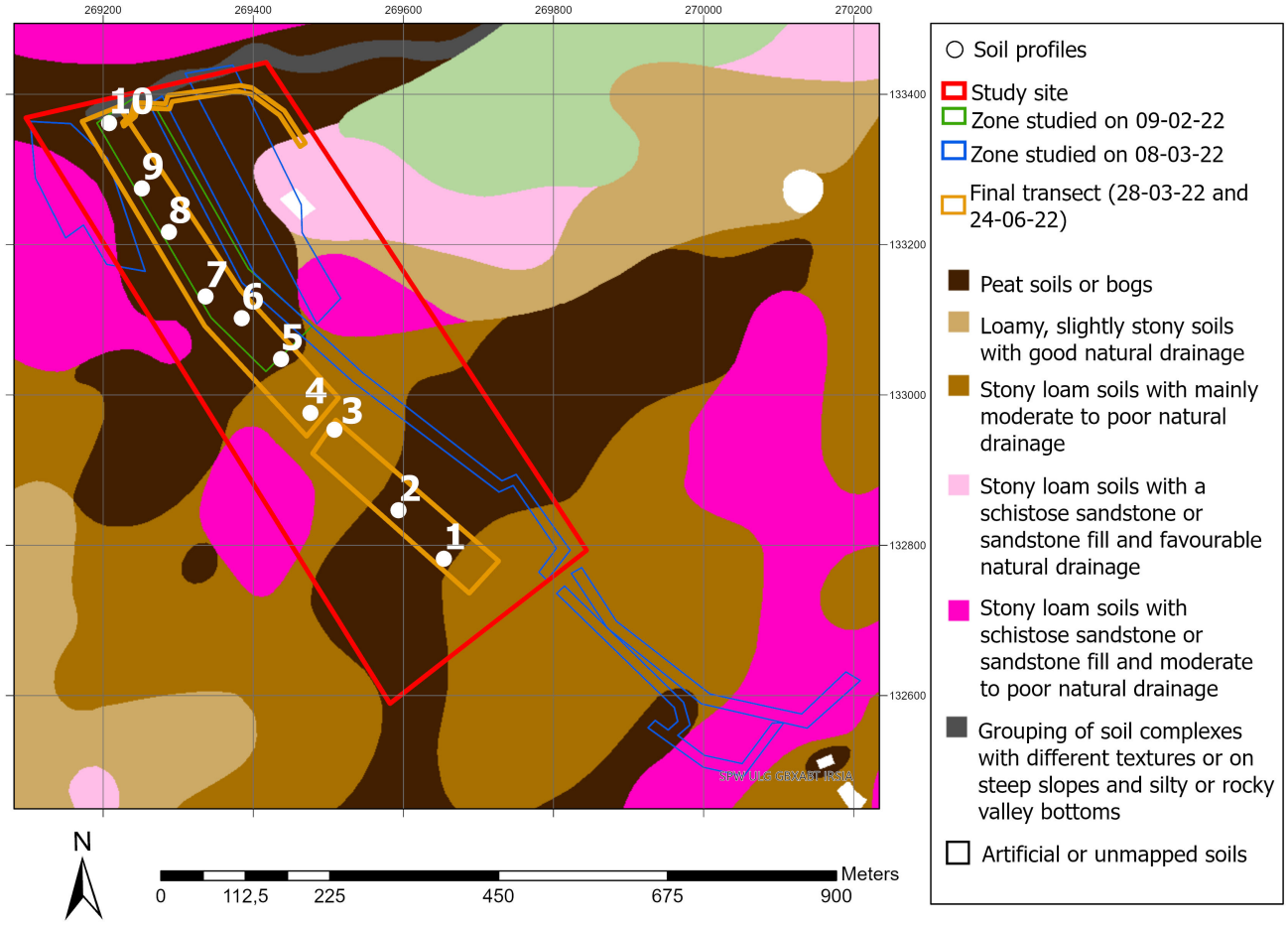

Figure 29: Pedology of each of the areas covered during the EMI measurement campaigns on February 9^{th}, March 8^{th}, March 28^{th} and June 24^{th} 2022, respectively as well as the 10 soil profiles realized on August 3^{rd} 2022

There seems to be a rough link between the stony loam area covered displayed in Figure 29 and the lower conductivity areas observed on the central plateau on the first three EMI measurement campaigns (Figure 18). One interesting observation from the two last maps from Figure 18 is the fact that there seems to be a continuity in the lower electrical conductivity values measured on the central plateau, extending across the road to the northern part of the southern plateau. This would coincide with the pedology map, as loam doesn't conduct electricity very well, it could be one of the causes that the electrical conductivity is lower in these loamy parts. This interpretation is however challenged by both the June measurement campaign (Figure 19), which doesn't show lower conductivities on the plateau, and the observations from March 8^{th}, represented by the blue outline on the above pedology map. The latter transect extends outside the study site perimeters for reasons mentioned in Section 6.1 but doesn't show any decrease in electrical conductivity when it reaches the second stony loam area on the south, it is actually the opposite, the electrical conductivity increases in that area (Figure 18).

The soil profiles realized on August 3^{rd} displayed in Figures 22 and 23 provided useful insight on the subsurface structure. They turned out to be fairly consistent with the pedology map. We can see that profiles 3 and 4 are both located in the "stony loam" area. These are also

the soil profiles that presented the thinnest layer of peat: 30 cm for 3 (Figure 22b) and 15 cm for profile 4 (Figure 23a). The thickness of the peat layer was more important in all other soil profiles, all reaching around 50 cm or more. Moreover, these are the only loam soils we observed on all the transects, except for profile 9, which showed clayey loam at a depth of 75 cm.

These profiles are punctual observations and proved to be of great help understanding the continuous measurement of the subsurface with the use of GPR. The representation of the radar studies that we have observed in Section 6.4 have revealed multiple layers below the surface. We could see some similarities between the different parts of the transect that are displayed in Section 6.4.1, 6.4.2, 6.4.3 and 6.4.4. Globally, we can observe 4 layers that are consistent on the whole length of the transect, even though the deeper layers may be more difficult to observe. The GPR imagery does, however, not allow to see what kind of material causes the reflection of the signal, thus the importance and usefulness of the soil profiles presented in Section 6.3. A first observation from the comparison of the soil profiles and the GPR images is that the depths of the deeper layers of the GPR imagery seem to be offset by 20 to 30 cm compared to the field observations (sometimes even more, depending on the water saturation). This is likely due to the transformation from the temporal level to the spatial level of the received signal of the GPR. Indeed, the dielectric permittivity value of the subsurface used during the transformation did not match the reality, hence the fact that the layers from the GPR images tend to appear deeper than in reality. A time-zero shift in the radar data may also have played a role in this offset.

Soil profile 2 has been made in the middle of GPR transect 3 (Figure 21) and its link with the GPR transect 3 has been discussed in Section 6.4.1. This soil profile was made trying to understand the slightly higher bulk electrical conductivity values measured on that location from Figures 18 and 19. As we can see in Figure 22a, the peat layer of profile 2 reaches 80 cm depth. Underneath, we can observe a blueish-gray clay layer, with a transition between peat and clay beginning around 60 cm depth and a pure clay layer at 80 cm depth. The presence of clay may play a role in the area's higher bulk electrical conductivity, as clay is a much better electrical conductor than loam [61, 64, 65]. However, soil profiles 5 (Figure 23b) and 6 present a similar structure, with an abrupt transition from peat to blueish-gray clay at 80 cm depth. These two last profiles are located on the central plateau, the area with the lowest measured bulk electrical conductivity of the site during the three first EMI measurement campaigns (Figure 18). Soil profiling only allows for a maximum depth of observation of 1 meter, it is possible that, in the case of profile 2, the clay layer reaches deeper. It is, however, difficult to prove, as the bedrock seems to have a fairly constant depth of around 2 m on most of the GPR images. Furthermore, the exact depth of the bedrock is not known because of the previously mentioned offset.

Soil Profile 3 (Figure 22b) has been made on the northern limit of the southern plateau (Figure 21), trying to understand its low conductivity seen in Figure 18. It may be partially explained by the loam layer located at 30 cm depth. Profile 4 (Figure 23a) presents a similar loam layer,

but once again, profiles 5 (Figure 23b) and 6 have both clay layers and have lower electrical conductivities during winter and early spring. This makes it difficult to link the conductivity to the loam content. The loam layer disappears between profile 3 (Figure 22b) and 2 (Figure 22a). This could be explained by the important slope observed in Figure 26, several meters before soil profile number 3. The layer may disappear around 80 meters, dipping in the depths as mentioned in Section 6.4.2. One other observation that may support this is the fact that the second layer observed at 50 cm depth before 70 meters seems to show a signal with more amplitude, suggesting that this layer is no longer loam.

Soil profile 7 was chosen after seeing a fairly exceptional peak around the 10 meters mark on segment 7 of GPR imagery, represented in Figure 28. This layer has been interpreted as being the bedrock, and soil profile 7 supports this idea. We can see in Figure 23c that around 55 cm depth, we reached a clayey layer with clearly visible slate fragments.

Figure 30 shows how the different horizons of the soil succeed to one another. The gray clay soil containing multiple slate fragments shown in Figure 31 is very likely the C horizon, where the alteration of the bedrock is still happening with visible bedrock fragments. These findings inform us that the bedrock is slate.

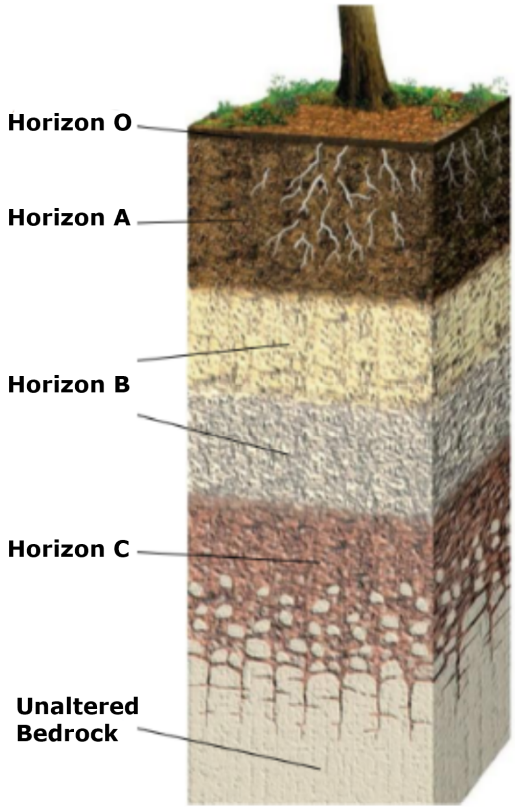

Figure 30: Succession of horizons in a soil profile [11]

Figure 31: Observed slate fragments from soil profile 7 (Figure 23c)

When observing Figure 28, we see that the main depth of the bedrock is around 2 meters, which shows an important rise, reaching its peak around 10 meters before dipping again at 2 meters depth. It rises again around 43 meters before dipping and disappearing at the 50 meters mark.

The other GPR images realized on the slope are unclear at deeper depths, making it harder to detect potential layers deeper beneath the surface. However, the 2-meter depth bedrock layer from GPR segment 7 (Figure 28) is visible on all GPR images south of this one (Figures 25, 26, 27). This fourth layer at about 2 m depth has thus been interpreted as being the bedrock in the discussed GPR imagery from Section 6.4. Comparison of this data from the top of the slope with the electrical conductivity measured in that same spot as illustrated in Figure 19 suggests that the bedrock has no visible influence on the electrical conductivity. Indeed, the GPR image clearly shows a dip in the bedrock depth right next to where the soil profile 7 was dug. There is, however, no noticeable electrical conductivity change around the place where the bedrock dips.

The soil profiling and GPR imagery have allowed for a more clear understanding of the soil subsurface of our study site, as well as its pedology. These two analysis techniques have proven to be complementary, the soil profiles having revealed an offset between the depths of the objects and layers displayed on the GPR imagery and in the reality. Although the site subsurface presents interesting heterogeneities, it remains difficult to establish a clear link between the solid phase properties and the measured electrical conductivity values displayed in Section 6.1. The clayey locations do not always show higher conductivity than the ones with loam, which seems contradictory. Low electrical conductivity values were measured on the central plateau during the three first EMI measurement campaigns (Figure 18), even though profiles 5 and 6 presented a very similar structure to profile 2, the location of the latter showed much higher conductivity values. These unexpected results as well as the observed changes between wetter and drier seasons suggest that the most important factor that influences the EMI results is related to seasonal influence.

7.3 Soil solution electrical conductivity

Drawing conclusions on the factors influencing the bulk electrical conductivity of the soil on the basis of the solid phase alone has proven to be difficult. The soil water electrical conductivity has thus been measured on June 24^{th} (Figure 20), the objective being to determine to what extent the water phase plays a role in the measured bulk electrical conductivity.

As shown by the map displayed in Figure 20, the soil solution conductivity ranges from 2,3 to 6,6 mS/m, which is lower than the bulk conductivity, which doesn't drop below 7 mS/m. This means that the liquid phase electrical conductivity (σ_w) is lower than the bulk surface conductivity (σ_s). During our three first campaigns realized throughout winter and early spring, the terrain was much more humid than in June, especially on the central plateau and on the edge of the southern one, where the conductivity values were low (Figure 18). We could observe that the soil in these two areas was saturated and water tended to accumulate on the surface, forming temporary ponds, whereas the rest of the field seemed drier.

One way to interpret the low conductivity values of the water is to link it with the melting of snow and precipitations during the winter and spring periods, as these added important quantities of water with a low concentration of electrolytes in the soils. The important rainfall

and the abundance of rivers originating from the region makes its waters relatively pure, which explains its low conductivity. The Polleur river has a higher conductivity than the soil water, with a measured value of 8,0 mS/m, which is low. We can link this to a low value of the σ_w parameter from Rhoade's relationship from Section 7.1. This parameter has been described by Walter et al. [55] and Comas et al. [75] as the parameter having the strongest influence on the bulk electrical conductivity σ of peat soils.

We believe that water plays an important role in the observed results. Even though we had not realized soil samplings during the winter, the analysis of the samples collected on June 24^{th} revealed that, even in early summer, the surface peat presented important water content. Four peat samples were made in June and revealed an average measured volumetric water content of 70%.

As we can see in Figure 32, it had rained a few days before the measurement campaigns of February 9^{th} and June 24^{th}. It had however not rained for several days before both of the campaigns realized in March. From a qualitative perspective, the soil was the wettest during the February and March studies, especially on the central plateau. The prolonged dry period following June 9^{th} (Figure 32) as well as the rising temperatures (Figure 33) may have played an important part in the drying of the central plateau, even though it rained on June 20^{th}, the soil water content was much more homogeneous on the whole transect, explaining why the measured electrical conductivity presented less variability.

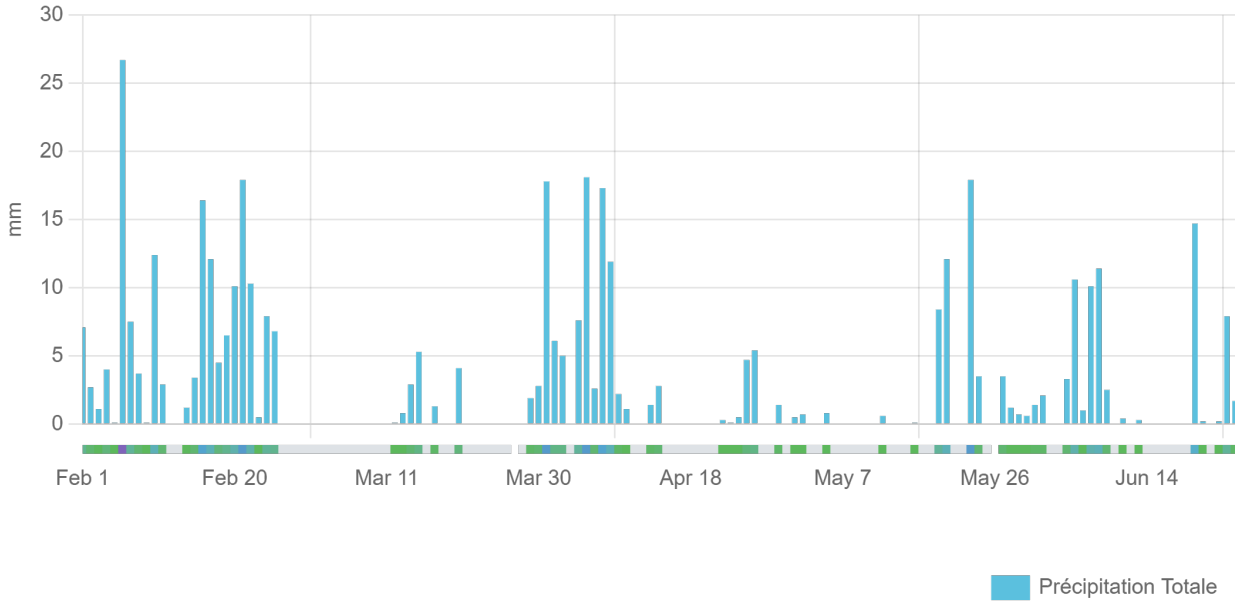

Figure 32: Rainfall registered on the Mont Rigi station between February and June 24^{th} [12]

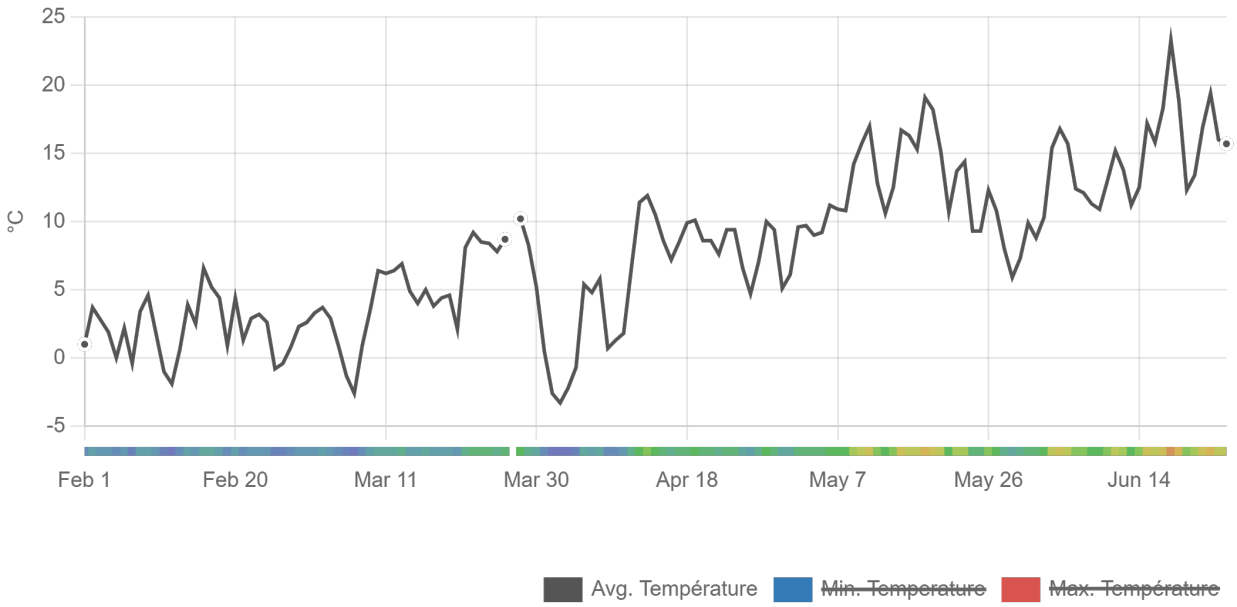

Figure 33: Temperature registered on the Mont Rigi station between February and June 24^{th} [12]

The trends observed in the EMI data from Section 6.1 were fairly consistent across all measurement campaigns within our study site. The only noticeable difference can be observed when comparing the results from the three first measurement campaigns with the fourth one that took place in June. Indeed, this last measurement campaign is the only time that the bulk electrical conductivity of the central plateau is similar to the ones measured on the rest of the study site. We can see in Figure 18 that the electrical conductivity of the central plateau was much lower than that of the rest of the site. Articles such as the ones written by Ponziani et al. in 2011 [76] and Theimer et al. in 1994 [79] describe a correlation between the electrical conductivity of the soil water and the bulk conductivity of the soil. In the experiment conducted by Ponziani et al. [76], the conductivity measured on peat samples strongly increased with the conductivity of the pore fluid. When the soil has a high water content, the conductivity decreases along with the water content. They, however, observed a threshold for σ_w at 10 mS/m under which the trend inverses: the bulk conductivity of the peat increased as the water content decreased. This seems to happen when the water conductivity σ_w is equal or lower than the solid phase conductivity σ_s. It seems to be the case in the situation of this study 20. As mentioned in Section 7.1, it has been observed by Walter et al. [55] that in the case of single-site approaches, it is the water content Θ that plays the most important part in σ. Another study conducted by Walter et al. in 2019 [78], concluded in their study that the electrical conductivity of drained peatlands, is much more sensitive to changes in water content at high saturation levels. This interpretation does not follow Rhoade's relationship (Equation 1), as this suggests that σ_s and σ_w are not independent in their influence on the bulk electrical conductivity σ.

This interpretation is coherent with our observations. As mentioned earlier, linking the bulk electrical conductivity heterogeneities across our site to water content Θ would explain the differences observed on the plateau across seasons. This would also explain why some clayey soils have low bulk electrical conductivities. It is likely that the drains and roads prevented

the water from flowing freely from one part of the study site to the adjacent ones, leading to an important accumulation of water on the central plateau, compared to the other areas. The hydrology of the site is however very disrupted, which makes the modelling of the water flows challenging at this time. However, continuous sensing on the site could be a valuable tool to better understand the hydrology on the site.

8 Conclusion

The objective of this master thesis is to better understand the subsurface critical zone using hydrogeophysical methods on a study site in the High Fens peatlands in Belgium. Peatlands are interesting biotopes because of the ecosystem services they provide, especially the important role they play in climate regulation. Aiming to better understand their subsurface with the use of non-invasive techniques is thus of significant importance for the future. This study has been done combining geophysical methods (EMI and GPR) with more traditional methods (direct soil water electrical conductivity measurements, soil profiling), allowing for a better understanding of the EMI and GPR data.

We chose to split the chosen site in three parts, on the basis of topography and hydrology disruptors. All parts of the site are disrupted by the fact the area has been intensely drained in the past in order to plant spruce trees. These spruce stands were cut down a few years ago, which caused more disruption in the soil structure. The drains are still mostly visible all across the study site and present a major disturbance to the surface and shallow hydrology of the site.

The bulk electrical conductivity measured by EMI on the study site is fairly low and is generally fairly homogeneous, ranging from 8,0 mS/m and 15,0 mS/m. Most values stay however between 10,0 mS/m to 13,0 mS/m. However, the measurements we made in winter and early spring showed that the plateau located in the middle of the study site did show on average lower bulk electrical conductivity values compared to the rest of the site, dropping as low as 4,0 mS/m. One other location tended to show a slightly higher conductivity, on the southern plateau of the study site, across all seasons.

The different factors influencing the bulk electrical conductivity of a soil have first been identified as being the solid and liquid phase of the soil. The discussion first focused on the importance of the solid phase in the measured electrical conductivity. The different GPR imagery observations, soil profiles and pedology maps have highlighted some heterogeneities in the soil structure across the subsurface of the site. These heterogeneities have however proven to be difficult to link with the observed bulk electrical conductivity. They are also incoherent with the seasonal changes observed on the conductivity of the plateau. Our electrical conductivity observations and their temporal evolution point to the fact that water content is the most important contributor to the changes of the bulk electrical conductivity of the soil. To assess this hypothesis, we realized soil water conductivity (σ_w) measurements, which revealed very low electrical conductivities, ranging from 2,3 mS/m to 6,6 mS/m. These very low soil solution conductivity values have been interpreted as being the reason why the bulk electrical conductivity (σ) of the most saturated zones were the lowest across the study site. Indeed, in the case of a low soil solution electrical conductivity, an increase in water content decreases the bulk electrical conductivity (σ). This has been observed when the soil water conductivity (σ_w) is inferior to the solid phase conductivity (σ_s). The roads and drains separating the three parts of the study site have acted as barriers, preventing the water from flowing freely from one part to another. This would explain why the central plateau retained more water than the rest of the study site during the wetter seasons, until a rise in temperature and a decrease in precipitation made the water table

level drop. This drop made the central plateau more similar to the two other areas in terms of water content. This would explain why the electrical conductivity measurements carried out in June showed more homogeneous values throughout the study site. However, the heavily disrupted hydrology makes it difficult to draw conclusions regarding water flows at this time.

This document should be used as a part of future peatlands studies, in order to further push the understanding of these biotopes. The results presented in this document will enable the LandSense project to choose the most interesting locations to place in-situ sensors. These will allow for a much more precise and continuous monitoring of the soil conditions, including water content and temperature. The findings of this master thesis present an interesting comparison point for the future drone-borne hydrogeophysical studies planned for the LandSense project.

9 Future perspectives

The LandSense project will be carried on for the next four years, which presents some opportunities to integrate the technologies and the results presented in this document with new ones to better understand peatlands.

Figure 34 illustrates the integration of different techniques in the CZ study. The next steps consist of the implementation of in-situ sensors in the field, which will provide continuous data about water content, temperature and electrical conductivity to a depth of up to one meter. These will enable continuous monitoring of the soil conditions, allowing for a better understanding of the evolution of soil conditions through time. The surface temperature will also be estimated by thermal infrared sensors.

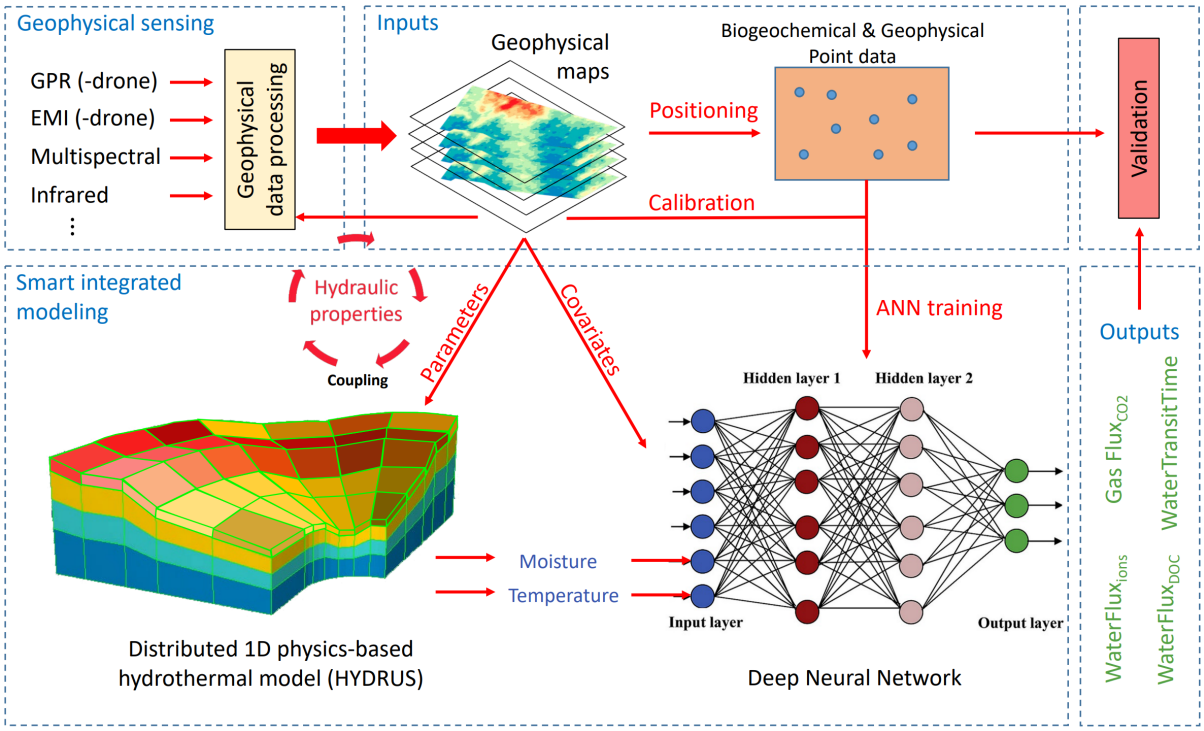

Figure 34: Concept of the integrated critical zone model [1]

The drone-borne GPR measurements mentioned in Section 5.4.3 were realized on June 24^{th} 2022, turned out to be unusable. One explanation may be caused by the low sensitivity of the radar measurements to electrical conductivity due to the high permittivity resulting from the very wet soil conditions. Another factor which probably affected the results is the fact that the drone-borne GPR measures the bulk electrical conductivity of the soil on an integrated depth of about 50 cm. The shallow soil layering of the study site may have caused a problem to the model, which assumed a homogeneous half-space medium. The use of a higher permittivity in the data processing may improve the quality of the data. As the drone-borne GPR are said to have a good correlation with EMI studies [73, 74], the EMI results from this document will serve as a basis for comparison.

Traditional measurements should also be realized in the form of a series of geochemical measurements. This will provide useful information about the soil parameters that will be used

during simulations later on by the Landsense project.

The findings of this document, such as the depth layering acquired by GPR and the homogeneous zones acquired by EMI, will serve as a basis for the calibration of the smart integration of the CZ. The end goal of the smart integration in the CZ is to "develop a new metamodeling framework of the CZ based on a smart combination of distributed physics-based model and a series of deep neural networks fed by massive geophysical data and geochemical analyses of point samples" [1]. This will be done by training an artificial neural network with data, thanks to a physics-based conceptual model (HYDRUS 1D).

References

[1] François Jonard, Sébastien Lambot, Sophie Opfergelt, Veerle Vanacker, and Kristof Van Oost. Pushing the boundaries of Critical Zone research: Unravelling hydrological controls on carbon and nutrient fluxes by integrating proximal sensing, field measurements and smart modelling. 2021.

[2] Where does gasoline go? | National Critical Zone Observatory. `https://czo-archive.criticalzone.org/national/blogs/post/where-does-gasoline-go/`.

[3] Kishor Aryal, Tek Maraseni, and Armando Apan. How much do we know about trade-offs in ecosystem services? A systematic review of empirical research observations. *Science of The Total Environment*, 806:151229, February 2022.

[4] Millennium Ecosystem Assessment (Program), editor. *Ecosystems and human well-being: synthesis*. Island Press, Washington, DC, 2005. OCLC: ocm59279709.

[5] European parliament and council. Eu soil strategy for 2030 reaping the benefits of healthy soils for people, food, nature and climate. `https://eur-lex.europa.eu/legal-content/EN/TXT/?uri=CELEX%3A52021DC0699`.

[6] L Robert Scholes, Montanarella and Nichole Brink Ben ten Anastasia Brainich, Barger. *The assessment report on land degradation and restoration: summary for policymakers*. Intergovernmental Science-Policy Platform on Biodiversity and Ecosystem Services (IPBES), Bonn, Germany, 2018. OCLC: 1244550463.

[7] Budiman Minasny, Örjan Berglund, John Connolly, Carolyn Hedley, Folkert de Vries, Alessandro Gimona, Bas Kempen, Darren Kidd, Harry Lilja, Brendan Malone, Alex McBratney, Pierre Roudier, Sharon O'Rourke, Rudiyanto, José Padarian, Laura Poggio, Alexandre ten Caten, Daniel Thompson, Clint Tuve, and Wirastuti Widyatmanti. Digital mapping of peatlands – A critical review. *Earth-Science Reviews*, 196:102870, September 2019.

[8] Angenot Ariane Jacquemart Anne-Laure. Un écosystème original, la tourbière. le cas des tourbières acides en belgique. *Probio revue*, 4:257–276, 2004.

[9] WalOnMap. `http://geoportail.wallonie.be/walonmap`.

[10] Ressources naturelles et Environnement Département de la Nature et des Forêts Direction de Malmédy SPW Agriculture. Study site history maps, n.d.

[11] Devos Elodie Lambert Richard Plume François Thomas Maxime Vandeuren Aubry Vincke Caroline Agnan Yannick, De Toffoli Marc. Lbir1336 - sciences du sol et excursions intégrées, 2020.

[12] meteostat.net. Météo mont-rigi. `https://meteostat.net/fr/station/06494?t=2022-02-01/2022-06-25`.

[13] Timothy White, Susan Brantley, Steve Banwart, Jon Chorover, William Dietrich, Lou Derry, Kathleen Lohse, Suzanne Anderson, Anthony Aufdendkampe, Roger Bales, Praveen Kumar, Dan Richter, and Bill McDowell. The Role of Critical Zone Observatories in Critical Zone Science. In *Developments in Earth Surface Processes*, volume 19, pages 15–78. Elsevier, 2015.

[14] Jón Örvar G. Jónsson and Brynhildur Davídsdóttir. Classification and valuation of soil ecosystem services. *Agricultural Systems*, 145:24–38, June 2016.

[15] Susan L. Brantley and Marina Lebedeva. Learning to Read the Chemistry of Regolith to Understand the Critical Zone. *Annual Review of Earth and Planetary Sciences*, 39(1):387–416, May 2011.

[16] Meltem Delibas, Azime Tezer, and Taneha Kuzniecow Bacchin. Towards embedding soil ecosystem services in spatial planning. *Cities*, 113:103150, June 2021.

[17] Raquel Granados Aguilar, Rebecca Owens, and John R. Giardino. The expanding role of anthropogeomorphology in critical zone studies in the Anthropocene. *Geomorphology*, 366:107165, October 2020.

[18] M. Sekhar, J. Riotte, L. Ruiz, J. Jouquet, and J. J. Braun. Influences of Climate and Agriculture on Water and Biogeochemical Cycles: Kabini Critical Zone Observatory. *Proceedings of the Indian National Science Academy*, 82(3), July 2016.

[19] John Dighton and Jennifer Adams Krumins, editors. *Interactions in Soil: Promoting Plant Growth*, volume 1 of *Biodiversity, Community and Ecosystems*. Springer Netherlands, Dordrecht, 2014.

[20] David Powlson. Will soil amplify climate change? *Nature*, 433(7023):204–205, January 2005.

[21] Rene Schils, Peter Kuikman, Jari Liski, Marcel Van Oijen, Pete Smith, Jim Webb, Jukka Alm, Zoltan Somogyi, Jan Van den Akker, Mike Billett, Bridget Emmett, Chris Evans, Marcus Lindner, Taru Palosuo, Patricia Bellamy, Robert Jandl, and Ronald Hiederer. Review of existing information on the interrelations between soil and climate change. (ClimSoil). Final report, December 2008.

[22] Shuai Ma, Liang-Jie Wang, Jiang Jiang, Lei Chu, and Jin-Chi Zhang. Threshold effect of ecosystem services in response to climate change and vegetation coverage change in the Qinghai-Tibet Plateau ecological shelter. *Journal of Cleaner Production*, 318:128592, October 2021.

[23] Josephine S. Head, Martha E. Crockatt, Zahra Didarali, Mary-Jane Woodward, and Bridget A. Emmett. The Role of Citizen Science in Meeting SDG Targets around Soil Health. *Sustainability*, 12(24):10254, January 2020.

[24] European Environment Agency (EEA). Land take and net land take — European Environment Agency. https://www.eea.europa.eu/data-and-maps/dashboards/land-take-statistics#tab-based-on-data, 2019.

[25] European Commission. Soil strategy. https://ec.europa.eu/environment/strategy/soil-strategy_en.

[26] Millennium Ecosystem Assessment. https://www.millenniumassessment.org/en/index.html.

[27] *Status of the world's soil resources: main report.* FAO : ITPS, Rome, 2015. OCLC: 945442780.

[28] Nigel Dudley and Sasha Alexander. *Global land outlook.* UNCCD, Bonn, Germany, first edition edition, 2017.

[29] European Soil Bureau Network. *Soil Atlas of Europe.* 2005.

[30] European parliament and council. Directive 2008/50/EC of the European Parliament and of the Council of 21 May 2008 on ambient air quality and cleaner air for Europe. http://data.europa.eu/eli/dir/2008/50/oj/eng, May 2008.

[31] European parliament and council. Directive 2000/60/EC of the European Parliament and of the Council of 23 October 2000 establishing a framework for Community action in the field of water policy. https://eur-lex.europa.eu/eli/dir/2000/60/oj, October 2000.

[32] European parliament and council. Biodiversity strategy for 2030. https://ec.europa.eu/environment/strategy/biodiversity-strategy-2030_en.

[33] Food and Agriculture Organization. Nos sols sont menacés. https://www.fao.org/3/mn997f/mn997f.pdf.

[34] UN Environment. Global environment outlook 4. https://www.unep.org/resources/global-environment-outlook-4, 2007.

[35] Science International Assessment of Agricultural Knowledge and Technology for Development. Agriculture at a crossroads. https://www.unep.org/resources/report/agriculture-crossroads-global-report, 2009.

[36] Ian Hannam and Ben Boer. *Drafting legislation for sustainable soils: a guide.* Number no. 52 in IUCN environmental policy and law paper. IUCN, Gland,Switzerland ; Cambridge, 2004. OCLC: ocm57213087.

[37] Kabindra Adhikari and Alfred E. Hartemink. Linking soils to ecosystem services — A global review. *Geoderma*, 262:101–111, January 2016.

[38] Région Wallonne. Décret relatif à la gestion des sols. https://wallex.wallonie.be/contents/acts/11/11938/1.html?doc=13358.

[39] Région Wallonne. 1er mars 2018 - décret relatif à la gestion et à l'assainissement des sols. http://environnement.wallonie.be/legis/solsoussol/sol006.htm.

[40] Région Wallonne. Le décret sols du 1er mars 2018. https://sol.environnement.wallonie.be/home/sols/presentation-generale-du-decret-sols-2018.html.

[41] Panos Panagos, Pasquale Borrelli, Jean Poesen, Cristiano Ballabio, Emanuele Lugato, Katrin Meusburger, Luca Montanarella, and Christine Alewell. The new assessment of soil loss by water erosion in Europe. *Environmental Science & Policy*, 54:438–447, December 2015.

[42] Directive of the european parliament and of the council establishing a framework for the protection of soil and amending directive 2004/35/ec, 2006.

[43] European parliament and council. Opinion of the european economic and social committee on the proposal for a directive of the european parliament and of the council establishing a framework for the protection of soil and amending directive 2004/35/ec, April 2007.

[44] European Commission. A European Green Deal. https://ec.europa.eu/info/strategy/priorities-2019-2024/european-green-deal_en.

[45] Ban Ki-Moon. UN Sustainable Development Goals: Blueprint for a Better Future. https://www.grips.ac.jp/en/single/pensee_sp1_ban/, March 2019.

[46] United Nations. Sustainable Development Goals. https://www.un.org/en/sustainable-development-goals.

[47] Gergely Tóth, Tamás Hermann, Manuela Ravina da Silva, and Luca Montanarella. Monitoring soil for sustainable development and land degradation neutrality. *Environmental Monitoring and Assessment*, 190(2):57, February 2018.

[48] Johan Bouma, Luca Montanarella, and Gregory Evanylo. The challenge for the soil science community to contribute to the implementation of the UN Sustainable Development Goals. *Soil Use and Management*, 35(4):538–546, December 2019.

[49] Afshin Asadi and Bujang B.K. Huat. Electrical resistivity of tropical peat. August 2017.

[50] Global Peatlands Initiative. What is the global peatlands initiative? https://www.globalpeatlands.org/#what_is_the_global.

[51] Virginia A Thorpe. Collaborative Study of the Cation Exchange Capacity of Peat Materials. *Journal of AOAC INTERNATIONAL*, 56(1):154–157, January 1973.

[52] Heli Saarikoski, Jyri Mustajoki, Turo Hjerppe, and Kaisu Aapala. Participatory multi-criteria decision analysis in valuing peatland ecosystem services—Trade-offs related to peat extraction vs. pristine peatlands in Southern Finland. *Ecological Economics*, 162:17–28, August 2019.

[53] Joachim G.C. Deru, Jaap Bloem, Ron de Goede, Harm Keidel, Henk Kloen, Michiel Rutgers, Jan van den Akker, Lijbert Brussaard, and Nick van Eekeren. Soil ecology and ecosystem services of dairy and semi-natural grasslands on peat. *Applied Soil Ecology*, 125:26–34, April 2018.

[54] Bjørn Kløve, Kerstin Berglund, Örjan Berglund, Simon Weldon, and Marja Maljanen. Future options for cultivated Nordic peat soils: Can land management and rewetting control greenhouse gas emissions? *Environmental Science & Policy*, 69:85–93, March 2017.

[55] J. Walter, E. Lück, A. Bauriegel, C. Richter, and J. Zeitz. Multi-scale analysis of electrical conductivity of peatlands for the assessment of peat properties: Electrical conductivity of peatlands. *European Journal of Soil Science*, 66(4):639–650, July 2015.

[56] R. Schumacker and C. Wastiaux. Topographie de surface et de subsurface des zones tourbeuses des réserves naturelles domaniales des Hautes-Fagnes - Rapport de synthèse. 2003.

[57] Freddy Damblon. Les depots tourbeux et l'histoire de la végétation sur le plateau des Hautes-Fagnes (Belgique), February 1996.

[58] Eric Goemaere, Simon Demarque, Roland Dreesen, and Pierre-Yves Declercq. The Geological and Cultural Heritage of the Caledonian Stavelot-Venn Massif, Belgium. *Geoheritage*, 8(3):211–233, September 2016.

[59] Froment Alfred. L'ancienne économie rurale de l'ardenne et son incidence sur la végétation des hautes fagnes. *Geoheritage*, 1968.

[60] Parc naturel Hautes Fagnes-Eifel. Plan de gestion du parc naturel hautes fagnes-eifel.

[61] Xin Li and Harry Vereecken, editors. *Observation and Measurement of Ecohydrological Processes*, volume 2 of *Ecohydrology*. Springer Berlin Heidelberg, Berlin, Heidelberg, 2019.

[62] Peter Styles Alireza Hajian. *Application of soft computing and intelligent methods in geophysics*. Springer Berlin Heidelberg, New York, NY, 2018.

[63] Yoram Rubin and Susan S. Hubbard, editors. *Hydrogeophysics*. Number v. 50 in Water science and technology library. Springer, Dordrecht [Netherlands] ; New York, 2005. OCLC: ocm60378951.

[64] Jonard François Lambot Sébastien. Lbres2101 - smart technologies in environmental engineering, 2021.

[65] James A. Doolittle and Eric C. Brevik. The use of electromagnetic induction techniques in soils studies. *Geoderma*, 223-225:33–45, July 2014.

[66] D. L. Corwin and S. M. Lesch. Application of Soil Electrical Conductivity to Precision Agriculture: Theory, Principles, and Guidelines. *Agronomy Journal*, 95(3):455–471, May 2003.

[67] K.A. Sudduth, N.R. Kitchen, W.J. Wiebold, W.D. Batchelor, G.A. Bollero, D.G. Bullock, D.E. Clay, H.L. Palm, F.J. Pierce, R.T. Schuler, and K.D. Thelen. Relating apparent electrical conductivity to soil properties across the north-central USA. *Computers and Electronics in Agriculture*, 46(1-3):263–283, March 2005.

[68] D. Altdorff, M. Bechtold, J. van der Kruk, H. Vereecken, and J.A. Huisman. Mapping peat layer properties with multi-coil offset electromagnetic induction and laser scanning elevation data. *Geoderma*, 261:178–189, January 2016.

[69] H. Abdu, D. A. Robinson, M. Seyfried, and S. B. Jones. Geophysical imaging of watershed subsurface patterns and prediction of soil texture and water holding capacity: GEOPHYSICAL IMAGING OF WATERSHED SUBSURFACE. *Water Resources Research*, 44(4), April 2008.

[70] François Jonard, Lutz Weihermüller, Harry Vereecken, and Sébastien Lambot. Accounting for soil surface roughness in the inversion of ultrawideband off-ground GPR signal for soil moisture retrieval. *GEOPHYSICS*, 77(1):H1–H7, January 2012.

[71] A.P. Annan. *GPR—History, Trends, and Future Developments*, volume 3 of *Subsurface Sensing Technologies and Applications*. Plenum Publishing Corporation, 1091 Brevik Place, Mississauga, Ontario L4W 3R7, Canada, October 2002.

[72] Jacob Fraden. *Handbook of modern sensors: physics, designs, and applications*. Springer, Cham Heidelberg New York Dordrecht London, fifth edition edition, 2016.

[73] Kaijun Wu, Gabriela Arambulo Rodriguez, Marjana Zajc, Elodie Jacquemin, Michiels Clément, Albéric De Coster, and Sébastien Lambot. A new drone-borne GPR for soil moisture mapping. *Remote Sensing of Environment*, 235:111456, December 2019.

[74] Kaijun Wu and Sebastien Lambot. Analysis of low-frequency drone-borne GPR for root-zone soil electrical conductivity characterization. *IEEE Transactions on Geoscience and Remote Sensing*, pages 1–1, 2022.

[75] Xavier Comas and Lee Slater. Low-frequency electrical properties of peat: LOW-FREQUENCY ELECTRICAL PROPERTIES OF PEAT. *Water Resources Research*, 40(12), December 2004.

[76] Michel Ponziani, E.C Slob, Ngan-Tillard D.J.M, and Heikki Vanhala. Influence of water content on the electrical conductivity of peat. June 2011.

[77] J. D. Rhoades, P. A. C. Raats, and R. J. Prather. Effects of Liquid-phase Electrical Conductivity, Water Content, and Surface Conductivity on Bulk Soil Electrical Conductivity. *Soil Science Society of America Journal*, 40(5):651–655, September 1976.

[78] J. Walter, E. Lück, C. Heller, A. Bauriegel, and J. Zeitz. Relationship between electrical conductivity and water content of peat and gyttja: implications for electrical surveys of drained peatlands. *Near Surface Geophysics*, 17(2):169–179, April 2019.

[79] Brian D. Theimer, David C. Nobes, and Barry G. Warner. A study of the geoelectrical properties of peatlands and their influence on ground-penetrating radar surveying1. *Geophysical Prospecting*, 42(3):179–209, April 1994.

Hydrogeophysical characterization of the soil along a floodplain-hillslope system in the High Fens

Sébastien Henrotte

Peatlands are biotopes of interest because of the numerous ecosystem services they provide such as water purification, biodiversity and carbon storage. The latter is especially important as even though peatlands only cover 3% of global land surface, they are estimated to contain between 5% and 20% of the global soil carbon stock.
In critical zone research, the integrated study of the subsurface on the landscape scale remains a key knowledge gap. This master thesis aims at addressing this problem by studying the subsurface of a hillslope-floodplain system in the High Fens peatlands with the use of hydrogeophysical methods: electromagnetic induction (EMI) and ground-penetrating radar (GPR).
The EMI measurements revealed electrical conductivity values ranging from 8,0 to 15,0 mS/m across the study site and showed some contrast between wet and dry seasons. GPR and soil profiling allowed us to better understand the subsurface structure, which does not show a direct link with the observed soil bulk electrical conductivity. Indeed, soil profiles with comparable structures presented very different electrical conductivities. Measurements of the soil solution electrical conductivity have revealed low values ranging from 2,3 mS/m to 6,6 mS/m. These values explain the lower bulk electrical conductivities measured in saturated zones.
The low soil water conductivity values, combined with the seasonal changes in measured bulk electrical conductivity, point to the fact that soil water content is the main contributor to the bulk electrical conductivity.
This master thesis is a good starting point for comparison with future integrated peatland subsurface studies as well as the use of hydrogeophysical techniques in such environments.

Université catholique de Louvain

Faculté des bioingénieurs

Croix du Sud, 2bte L7.05.01, 1348 Louvain-La-Neuve, Belgique | www.uclouvain.be/agro